

800268

AFOSR-66-1847

R-6654

EFFECTS OF ALUMINUM ON SOLID-PROPELLANT  
COMBUSTION INSTABILITY

By

C. L. Oberg  
A. L. Huebner

July 1966

Sponsored By  
The Air Force Office of Scientific Research  
Under  
Contract AF49(638)-1575

3. Each transmittal of this document outside the agencies of the  
U. S. Government must have prior approval of AFOSR (SRGL).



**ROCKETDYNE**  
A DIVISION OF NORTH AMERICAN AVIATION, INC.  
6633 CANOGA AVENUE, CANOGA PARK, CALIFORNIA

[Redacted stamp area]

**ROCKETDYNE**  
A DIVISION OF NORTH AMERICAN AVIATION, INC.  
6633 CANOGA AVENUE, CANOGA PARK, CALIFORNIA

AFOSR-66-1847

9

R-6654

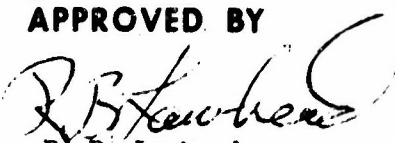
EFFECTS OF ALUMINUM ON SOLID-PROPELLANT  
COMBUSTION INSTABILITY

Sponsored By  
The Air Force Office of Scientific Research  
Under  
Contract AF49(638)-1575  
G.O. 8721

**PREPARED BY**

C. L. Oberg and A. L. Huebner  
Research Division  
Rocketdyne Engineering  
Canoga Park, California

**APPROVED BY**



R. B. Lawhead  
Section Chief

Propulsion Processes and Applications

NO. OF PAGES 98 & xi

REVISIONS

DATE 30 July 1966

DATE	REV. BY	PAGES AFFECTED	REMARKS



ROCKETDYNE • A DIVISION OF NORTH AMERICAN AVIATION, INC.

**FOREWORD**

This technical report was prepared for the Director of Aerospace Sciences, Air Force Office of Scientific Research, Washington, D. C., in completion of Contract AF49(638)-1575. It describes research studies carried out by the Physical Processes Group of the Research Division of Rocketdyne, a Division of North American Aviation, Inc.



ROCKETDYNE • A DIVISION OF NORTH AMERICAN AVIATION, INC

## ABSTRACT

An analytical and experimental program to investigate the effects of aluminum on solid-propellant combustion instability was conducted. The analytical phase was devoted to a determination of the energy dissipation rate associated with possible damping mechanisms at either the burning propellant surface or in the chamber volume. Particulate damping, droplet deformation, surface modes of vibration, the effects of aluminum on the shattering; and combustion interaction of the burning surface with the acoustic field were all considered. The relative magnitude of these damping mechanisms are developed and discussed.

The effects of aluminum on nonacoustic instability were also considered in the analytical phase. It was shown that the nonacoustic problem could be treated by employing conventional acoustic methods, taken to an appropriate limit. This treatment was applied to various existing experimental data on nonacoustic instability, and good agreement was obtained. This information was used to propose a mechanism for quasi-periodic shedding of aluminum from the burning surface.

This analysis was followed by an experimental phase having the goal of separating energy dissipation mechanisms into surface and chamber-volume effects and establishing the relative magnitudes of each. These measurements were made employing a T-burner in which a pressure pulse could be generated. Measurements were made on propellants containing up to 15-percent aluminum at mean-pressure levels up to 600 psi and over a frequency range of 200 to 2000 cps. A discussion is presented of the results of these experiments, particularly with respect to the damping mechanisms considered in the analysis. Some information applicable to nonacoustic instability was obtained as well.



ROCKETDYNE • A DIVISION OF NORTH AMERICAN AVIATION, INC.

## CONTENTS

<b>Foreword</b>	iii
<b>Abstract</b>	v
<b>Introduction and Summary</b>	1
<b>Analysis</b>	5
Particulate Damping	6
Energy Dissipation by Deformation of Droplets on the Burning Surface	14
Energy Dissipation in the Surface Modes of a Droplet	16
Dissipation by Periodic Droplet Shattering	16
Effects of Aluminum on Combustion Interaction of the Burning Surface	18
The Effects of Aluminum on Nonacoustic Instability	23
<b>Experimental Study</b>	27
Experimental Approach	27
Experimental System	28
Experimental Results	33
<b>Conclusions and Recommendations</b>	53
<b>References</b>	57
<b>Publications Resulting From Work Performed</b>	63
<b>Appendix A</b>	
Nomenclature	A-1
<b>Appendix B</b>	
Analysis of Nonacoustic Instability	B-1
<b>Appendix C</b>	
Experimental Data	C-1



ROCKETDYNE • A DIVISION OF NORTH AMERICAN AVIATION, INC.

## ILLUSTRATIONS

1. Comparison of Epstein-Carhart and Temkin Results for Particulate Damping . . . . .	10
2. Comparison of Total Damping and Viscous Contribution According to Temkin Equations . . . . .	11
3. Particulate Damping in Terms of the Temporal Damping Constant According to Epstein-Carhart Theory . . . . .	12
4. Sketch of the Pulsed T-Burner . . . . .	29
5. Decay-Rate Data for A-Propellant at 200 psi . . . . .	36
6. Decay-Rate Data for C-Propellant at 200 psi . . . . .	37
7. Decay-Rate Data for P-4 Squibs at 200 psi . . . . .	39
8. Comparison of Experimentally Determined Particulate Damping With Constant Particle-Size Curves for C-Propellant at 200 psi . . . . .	
9. Decay-Rate Data for A-Propellant at 600 psi . . . . .	41
10. Decay-Rate Data for C-Propellant at 600 psi . . . . .	43
11. Decay-Rate Data for P-4 Squibs at 600 psi . . . . .	44
12. Comparison of Experimentally Determined Particulate Damping With Constant Particle-Size Curves for C-Propellant at 600 psi . . . . .	45
13. Decay-Rate Data for A-Propellant at 400 psi . . . . .	46
14. Decay-Rate Data for P-4 Squibs at 400 psi . . . . .	47
15. Decay-Rate Data for B-Propellant at 200 psi . . . . .	48
16. Decay-Rate Data for B-Propellant at 400 psi . . . . .	49
17. Decay-Rate Data for B-Propellant at 600 psi . . . . .	50
18. Experimental Concentration Dependence of the Particulate Damping for B- and C-Propellant at 200 psi and 1000 cps . . . . .	52



ROCKETDYNE • A DIVISION OF NORTH AMERICAN AVIATION, INC.

TABLES

1. Number of Drops in Gas Volume Relative to Number of Drops on Burning Surface . . . . .	20
2. Weighted Rate of Energy Dissipation Due to Particulate Damping . . . . .	20
3. Rate of Energy Dissipation Due to Droplet Deformation . . . .	21
4. Composition of Propellants Used . . . . .	32



ROCKETDYNE • A DIVISION OF NORTH AMERICAN AVIATION, INC.

## INTRODUCTION AND SUMMARY

Combustion instability has persisted as a problem in motor development programs for many years. The addition of powdered metals has been found to be highly effective in suppressing acoustic, or high-frequency, instability. Aluminum, in particular, is the principle means of suppressing this form of instability, but the presence of aluminum appears to intensify nonacoustic-instability problem. In spite of its extensive use, the mechanisms by which aluminum operates as a stabilizing influence are not well understood. (Ref. 1 through 3).

One mechanism suggested for the stabilizing influence of aluminum is the damping associated with the condensed phase products of the aluminum combustion. The known effectiveness of particulate damping indicates that this mechanism must play an important, if not dominant, role, also, interaction of the aluminum with the combustion has been suggested as a stabilizing influence (Ref. 1 through 8). Experimental evidence has been cited for both of these effects but, except in one instance, no definitive answers have evolved.

For low aluminum concentrations, at least for one propellant system and for up to 1.5 weight-percent of aluminum, particulate damping has been found to be dominant (Ref. 6 and 7). However, practical propellants frequently contain 10- to 20-percent aluminum. At these loadings the balance between particulate damping and other damping mechanisms may be completely shifted. To use powdered metals most effectively to promote stability, the stabilizing processes must be better understood. With this motivation, a research program was undertaken to investigate the effect of aluminization on solid propellant combustion, and in particular, to differentiate between surface and chamber-volume effects in damping or driving combustion oscillations.



ROCKETDYNE • A DIVISION OF NORTH AMERICAN AVIATION, INC.

The initial phases of the program were theoretical. Various processes were investigated in an effort to estimate analytically their relative importance, within each of the categories cited (surface and chamber-volume effects), as well as with respect to each other. In some cases these estimates could be made on the basis of a fairly well-defined theory. In others the complexity and lack of understanding of the mechanism, particularly in the combustion environment, made estimates highly uncertain.

Particulate damping was found to be a strong dissipative factor, particularly at high frequency. Droplet deformation was completely insignificant. The contribution due to surface modes of vibration was larger than that for droplet deformation, but in absolute magnitude was also insignificant. In the absence of experimental data concerning the shattering of drops near the burning surface, as well as a model for their subsequent behavior, droplet shattering as a dissipative mechanism could only be bracketed between wide limits, with the upper limit of significant relative magnitude. The effects of aluminum on combustion interaction of the burning surface with the acoustic field was found to be a completely intractable problem within the scope of the present program; in consequence, no quantitative estimate of its associated energy dissipation rate could be made.

In addition, the effects of aluminum on nonacoustic instability were considered. An investigation of nonacoustic instability produced several results of considerable importance, although not necessarily with respect to the role of aluminum. Analysis showed that the nonacoustic problem could be developed using conventional acoustic methods with the nonacoustic mode being a zeroth-longitudinal acoustic mode for the cavity. With this basis, an acoustic instability combustion model was applied to the description of the nonacoustic instability data reported by several investigators.



ROCKETDYNE • A DIVISION OF NORTH AMERICAN AVIATION, INC.

Highly satisfactory agreement was obtained. Finally, the information developed was applied to the effects of aluminum in the nonacoustic frequency range to propose a source of the periodicity in aluminum shedding observed in experimental investigations.

The results of the analytical task made the need for experimental measurements evident. A method was needed to measure the combustion response (response function) of the burning surface for a highly aluminized propellant. Secondly, any changes in the response function needed to be compared to the particulate damping for that propellant to assess the importance of these changes in the response function. Therefore, measurements of the particulate damping were also needed. These measurements were made employing a T-burner in which a pressure pulse could be generated. Although this method was not fully satisfactory with respect to the accuracy obtainable, there is at present no other method capable of producing the necessary information. Using this technique, measurements were made on propellants containing up to 15-percent aluminum at mean-pressure levels to 600 psi and over a frequency range of 200 to 2000 cps.

Satisfactory results were obtained. It was found that particulate damping was the dominant stabilizing mechanism. Measurable particulate damping was obtained even at the lowest frequencies. The response function did not appear to be greatly altered by the presence of aluminum; however, the data consistently indicated that the aluminized burning surface is more unstable than the corresponding unaluminized surface. In spite of limitations of the experimental method, the consistency of the data suggests that the conditions exist. These results are of considerable importance because they represent the only data available for highly aluminized propellants.



## ANALYSIS

A number of phenomena may be cited as possible mechanisms by which inclusion of aluminum powder in a solid propellant formulation introduces energy sources or sinks during unstable combustion. For some of these (e.g., particulate damping) indications existed before initiation of the reported study that their role was important. In most cases, however, no evidence existed.

In the first phase of the investigation, the following possible mechanisms of damping were considered analytically:

1. Particulate damping
2. Deformation of droplets at the burning surface
3. Droplet surface modes
4. Droplet shattering
5. Combustion interaction

For each of these it was attempted to develop a quantitative expression for the change of energy-with-time associated with the mechanism. The occurrence of some of these phenomena (e.g., droplet shattering) in the vicinity of the burning surface considerably complicates the analysis. If the latter is to be kept within the bounds of tractability, simplifications are necessary which sometimes lead to results which are valid only as order of magnitude calculations.

Subsequently, weighting factors were calculated for each mechanism so that direct comparison could be made. This required specific assumptions to be

PRECEDING PAGE BLANK



ROCKETDYNE • A DIVISION OF NORTH AMERICAN AVIATION INC

made concerning, in particular, the ratio of the number of aluminum droplets on the burning propellant surface to those in the product-gas volume. It was then possible to directly estimate the relative influence of the dissipation factors considered. In spite of the approximations made, in most cases contributions differ by a great enough amount to permit clear resolution of this relative influence. Where this resolution has not been possible by the analytical techniques described in this section, further evidence on damping was obtained from the experimental phase of the program.

#### PARTICULATE DAMPING

Particulate damping is indicated as a major effect in the role played by powdered aluminum in suppressing acoustic instability. Consequently, it is convenient to discuss this process first and use it as a basis for comparison with the contributions of other damping processes. For these reasons, as well as its greater tractability than many of the mechanisms treated subsequently, particulate damping has been analyzed in considerable detail.

The theory of particulate damping has been analyzed by Sewell (Ref. 9), Lamb (Ref. 10), Epstein and Carhart (Ref. 11), Blair (Ref. 12), Chow (Ref. 13), Soo (Ref. 14), and most recently by Temkin (Ref. 15). The results of these investigations appear to be essentially in agreement with the exception of Soo (Ref. 14). Soo finds a small difference (about a factor of two) between his results and those of Epstein-Carhart (Ref. 11) for a particular numerical example. However, Soo's model is equivalent to that of Temkin (Ref. 15) over the range of interest but, contrary to Soo, Temkin finds excellent numerical agreement between his results and the Epstein-Carhart results. In the current investigation, the Temkin analysis



ROCKETDYNE • A DIVISION OF NORTH AMERICAN AVIATION, INC

was verified and excellent numerical agreement was also found with the Epstein-Carhart results. Therefore, the disparity was discounted as unimportant. In the current program the Epstein-Carhart equations were used for most calculations. The Temkin equation was used for comparative purposes and for some calculations.

The theory has had substantial experimental verification, although the data are limited. The data of Zink and Delsasso (Ref. 32) agree very well with Epstein-Carhart theory, over the range in which data were obtained. The recent data of Temkin and Dobbins (Ref. 33) agree very well with the Temkin treatment (and, presumably, Epstein-Carhart theory as well) over a broad range of conditions. Earlier data by Dobbins and Temkin (Ref. 34) also agree with Epstein-Carhart theory. Therefore, it appears that particulate damping is rather well understood.

The most well-known analysis of particulate damping is the theory of Epstein and Carhart (Ref. 11). They have solved the wave-scattering problem for a plane wave impinging upon a single droplet, including viscous and thermal effects. The time-average rate of energy dissipation was then calculated from the rate of entropy generation in the entire volume, both within and without the sphere. The assumption was made that the rate of dissipation for many droplets may be found by adding the dissipation rate for each droplet. Thus they calculate an attenuation coefficient for an aerosol. The reduced attenuation coefficient is given by (Ref. 34):

$$\frac{a_0 \alpha}{c_m \omega} = \bar{\alpha} = \delta \left\{ \frac{9}{4} (1 + y) F(y) + \frac{3(\gamma - 1)}{2 Pr} (1 + Pr^{1/2} y) G(y) \right\} (1)$$



ROCKWELL INTERNATIONAL • A DIVISION OF NORTH AMERICAN AVIATION, INC.

where

$$F(y) = \frac{16y^2}{16y^4 + 72\delta y^2 + 81\delta^2(2y^2 + 2y + 1)} \quad (2)$$

$$G(y) = \frac{\Pr y^2}{\Pr^2 y^4 + 2\left(\frac{3}{2}\delta\frac{c_p'}{c_p}\right)\Pr^{3/2} y^3 + \left(\frac{3}{2}\delta\frac{c_p'}{c_p}\right)^2} \quad (3)$$

The nomenclature is shown in Appendix A.

The approach taken by Temkin (Ref. 15) is rather different from that used by Epstein and Carhart. He writes the conservation equations for a particle-laden gas. The assumptions were made that Stoke's law may be used to describe the force on a particle and, secondly, that the heat transport to a particle may be described by the expression for heat conduction to a sphere in a stagnant fluid. The linearized conservation equations were solved for one-dimensional behavior. For very small mass concentrations of particles, he finds:

$$\bar{\alpha} = \frac{\omega \tau_d}{1 + \omega \tau_d} + (\gamma - 1) \left( \frac{c_p'}{c_p} \right) \frac{\omega \tau_t}{1 + \omega^2 \tau_t^2} \quad (4)$$

If the thermal dissipation is negligible relative to the viscous dissipation, then for finite mass concentrations

$$\bar{\alpha} = \frac{\omega \tau_d}{1 + \omega \tau_d} \left\{ 1 - \frac{C_m}{2(1 + \omega^2 \tau_d^2)} \right\} \quad (5)$$

Detailed calculations were made with both the Epstein-Carhart equation and the Temkin equation as noted above. A numerical example for low



ROCKETDYNE • A DIVISION OF NORTH AMERICAN AVIATION INC

concentrations as calculated by each equation is shown in Fig. 1. The calculations were made for  $\text{Al}_2\text{O}_3$  droplets suspended in combustion gases. The numerical agreement is very good except at large values of  $y$ , i.e.,  $(\frac{\omega r^2}{2\nu})^{1/2}$ . Perhaps the disparity in this region can be attributed to deviations from the simple Stokes-law drag relationship expected in the region. Fortunately, the Temkin equation is adequate for the combustion-instability case since the particle sizes encountered are small.

In Fig. 2 numerical comparison is shown between the viscous contribution and the total reduced damping coefficient as calculated by the Temkin equation. It is apparent that the thermal contribution is small for this case. Experimentally, in combustion instability studies, the temporal attenuation coefficient is the quantity usually measured. The Epstein-Carhart curve shown in Fig. 1 has been converted to such a coefficient and the results are plotted in Fig. 3 for several particle sizes and a mass ratio,  $C_m$ , of one-tenth. In these terms the effectiveness of particulate damping is very apparent.

It is useful, in the discussion of experimental results, to consider the mean particle size to be used in these equations if a distribution of particle sizes is present. The mass ratio,  $C_m$ , may be estimated from the propellant composition and, therefore, is presumed to be known. The thermal contribution is assumed to be negligible. It is simplest to deal with the Temkin equation; the Epstein-Carhart equation is dealt with in an identical manner. Integrating over the size distribution, it is found that

$$\frac{C_m k_1 \bar{r}^2}{1 + k_1^2 \bar{r}^4} = \left( \frac{4\pi \omega \rho_t}{3 a_0 g} \right) \int_0^\infty \frac{k_1 r^5 dn}{1 + k_1^2 r^4} \quad (6)$$



ROCKETDYNE • A DIVISION OF NORTH AMERICAN AVIATION, INC.

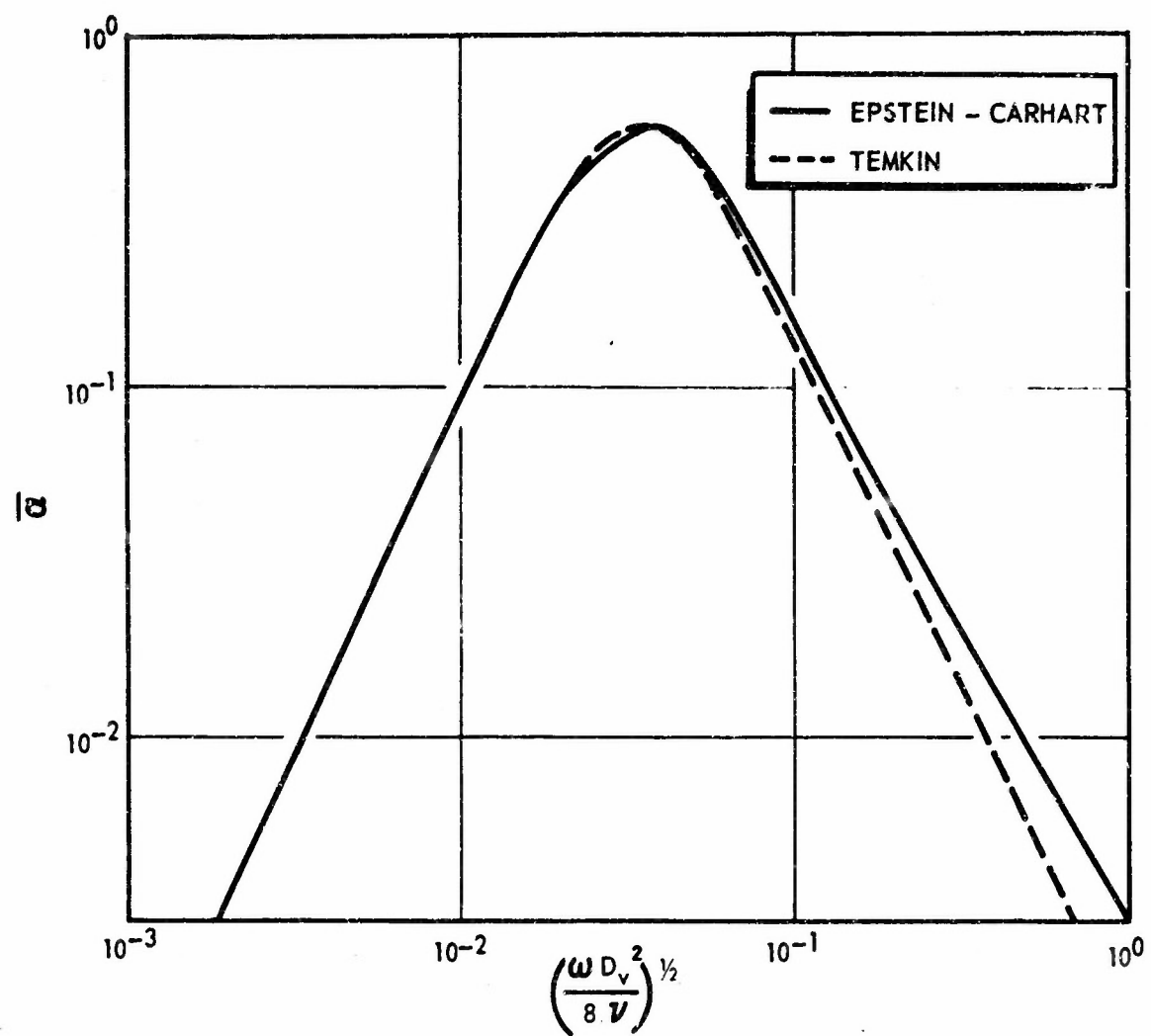


Figure 1. Comparison of Epstein-Carhart and Temkin Results for Particulate Damping



ROCKETDYNE • A DIVISION OF NORTH AMERICAN AVIATION, INC.

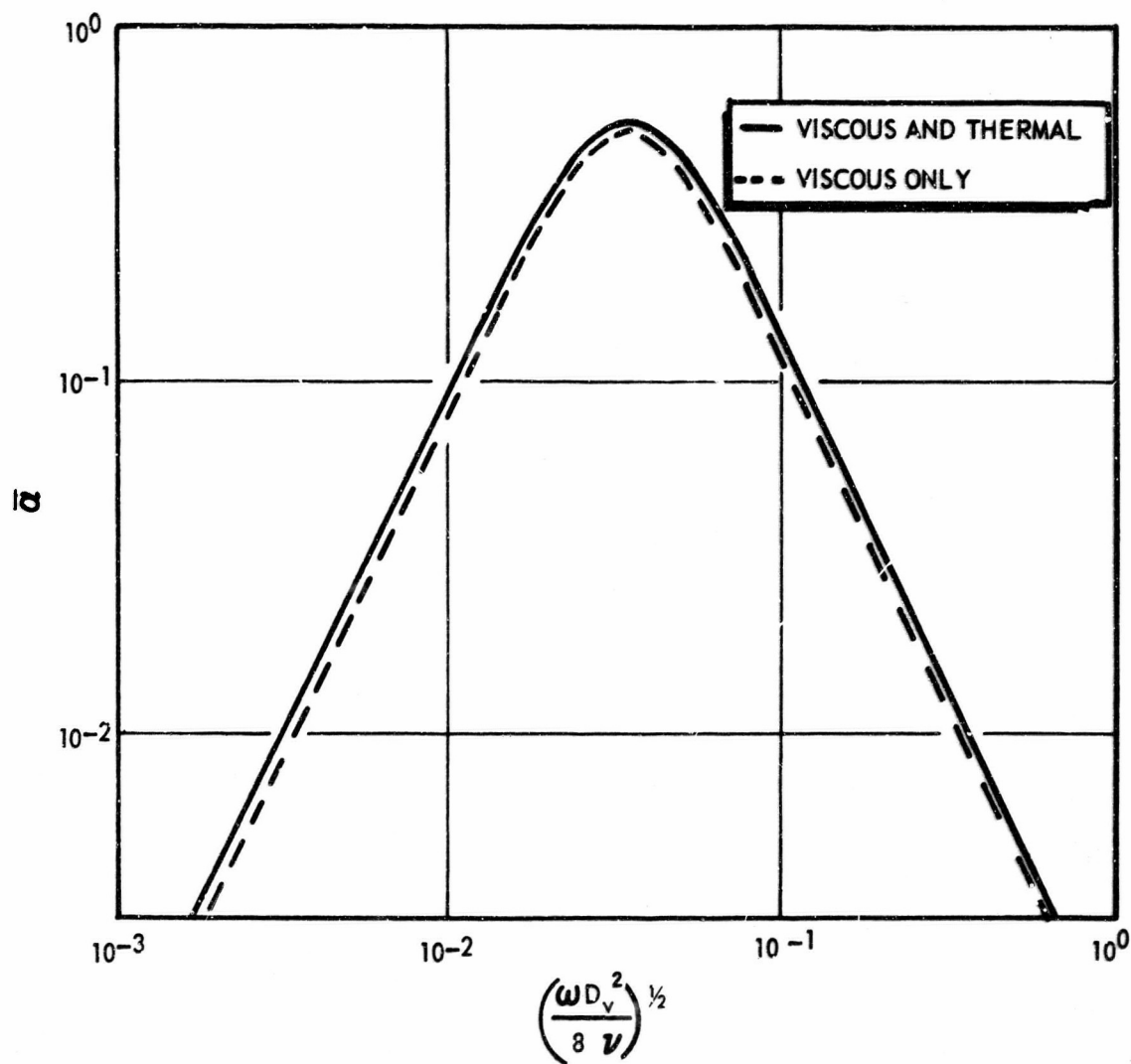


Figure 2. Comparison of Total Damping and Viscous Contribution According to Temkin Equations



ROCKETDYNE • A DIVISION OF NORTH AMERICAN AVIATION, INC.

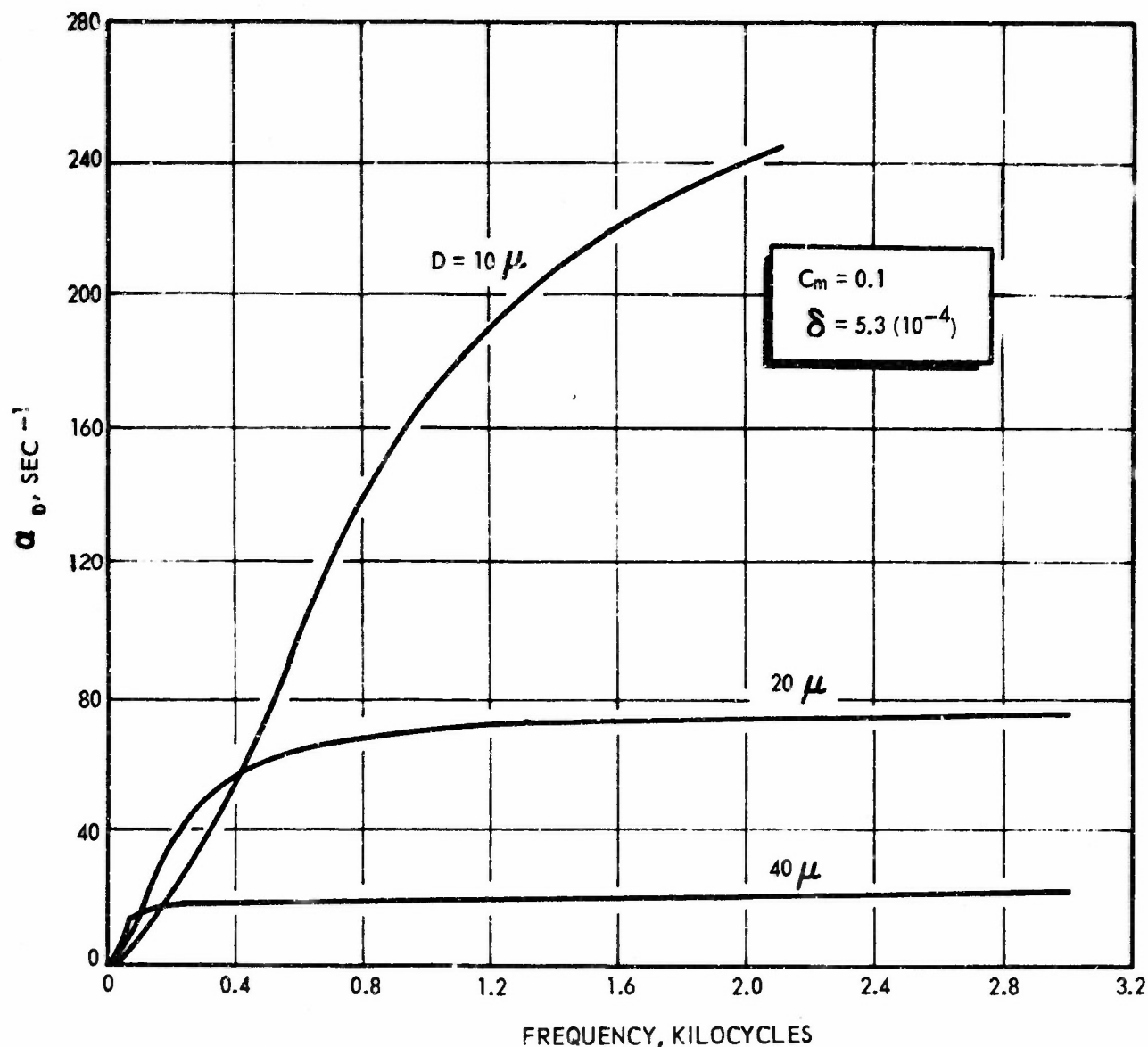


Figure 3. Particulate Damping in Terms of the Temporal Damping Constant According to Epstein-Carhart Theory



ROCKETDYNE • A DIVISION OF NORTH AMERICAN AVIATION, INC.

where

$$k_1 = \frac{2 \omega \rho_l}{9 \mu} \quad (7)$$

and

$$C_m = \frac{4 \pi \rho_l}{3 \rho_g} \int_0^\infty r^3 dn \quad (8)$$

Two simple cases occur. If the distribution is such that the integrand is negligible for large sizes, i.e., the integrand is non-negligible for  $k_1^2 r^4 \ll 1$ , then

$$\bar{r}^2 = \frac{\int_0^\infty r^5 dn}{\int_0^\infty r^3 dn} \quad (9)$$

with the definition

$$D_{ij}^{(i-j)} = \frac{\int_0^\infty D^i dn}{\int_0^\infty D^j dn} \quad i, j = 0, 1, 2, 3, \dots \quad (10)$$

it is apparent that the  $D_{53}$  mean diameter is appropriate for small particles.

If the integrand is non-negligible for  $k_1^2 r^4 \gg 1$ , then the  $D_{31}$  mean diameter is found for large particles. From the Epstein-Carhart equation it is also found that  $D_{53}$  should be used for small particles,  $D_{31}$  for large particles, and  $D_{32}$  for very large particles. These considerations were used in examining the experimental results discussed below.



ROCKETDYNE • A DIVISION OF NORTH AMERICAN AVIATION, INC

The rate of energy dissipation due to particulate damping may be obtained rather directly. Assuming the thermal contribution to be negligible, it was found from the Epstein-Carhart theory that, for each particle,

$$\dot{E}_{\text{part}} = 3 \pi r \mu (1 + y) y^2 F(y) \quad (11)$$

for small particles, this reduces to

$$\dot{E}_{\text{part}} = \frac{4 \pi r^5 \omega^2}{27 \nu \delta^2 \rho a_0^2} \hat{p}^2 \quad (12)$$

where  $\hat{p}$  is the amplitude of the incident pressure wave. Equation 12 will be used to make comparisons for specific cases after expressions have been described for other dissipative processes.

#### ENERGY DISSIPATION BY DEFORMATION OF DROPLETS ON THE BURNING SURFACE

Perhaps the simplest technique available for calculation of the rate of degradation of acoustic energy is described by Landau and Lifshitz (Ref. 17). From consideration of the rate of entropy generation, they obtain the following expression:

$$\dot{E} = - < \left\{ \frac{k}{T_0} \int_v (\nabla T)^2 dv + \mu \int_v \Phi_v dv \right\} > \quad (13)$$

where the integration is carried out over the entire volume and  $< >$  indicates a time average. The convenience of Eq. 13 is that  $\dot{E}$ , to a first approximation, can be calculated from the solutions to the acoustic problem



ROCKETDYNE • A DIVISION OF NORTH AMERICAN AVIATION, INC.

with losses neglected, since the losses contribute only second-order effects in general. This approximation was used to calculate the dissipation in the various oscillatory modes of a droplet. A similar approximation was used by Cantrell (Ref. 18).

Two cases were considered: (1) a drop located near a velocity node and (2) a drop exposed to a transverse acoustic velocity. In each case the drop was approximated as spherical. In the first case, only radial behavior need be considered. No problem is encountered in attaining a solution to the wave equation for this case. The viscous contribution to the dissipation was found to be

$$\dot{E}_{vis} = 16 \pi \mu_\ell D_s \left[ 1 - \frac{\left( \frac{\omega}{c_\ell} D_s \right)^2}{36} \right] \frac{p^2}{\rho_\ell^2 c_\ell^2} \quad (14)$$

where terms smaller than  $\left( \frac{1}{2} \frac{\omega}{c_\ell} D_s \right)^2$  have been dropped. The thermal contribution was found to be

$$E_{therm.} = \frac{k_\ell}{4 \mu_\ell} \left( \frac{\alpha_\ell}{\beta_\ell} \frac{\gamma_\ell - 1}{\gamma_\ell} \right)^2 \quad \dot{E}_{vis} \approx 10^{-4} \dot{E}_{vis} \quad (15)$$

which is negligible. Eq. 14 will be used later for specific cases.

For the droplet exposed to a transverse acoustic velocity, some difficulty was found in handling the velocity distribution in the boundary layer. This distribution was finally handled in an approximation. A solution was obtained in a manner similar to that used by Rayleigh (Ref. 19). The solution was found to exhibit predominantly radial motion, the nonradial portion of the solution being on the order of  $10^{-6}$  times the radial portion. This result may be due to the imposed approximations; however, on the basis of the approximate computation, it was concluded



ROCKETDYNE • A DIVISION OF NORTH AMERICAN AVIATION, INC

that the contribution to the dissipation was of the same order as that found for a drcp located near a velocity node.

#### ENERGY DISSIPATION IN THE SURFACE MODES OF A DROPLET

The resonant frequencies for aluminum droplets oscillating in their lowest surface modes are in the range of instability frequencies of interest, for not unreasonably large droplets. This suggests that a high dissipation may be obtained from those droplets. The dissipation rate was again calculated employing Eq. 13 .

The solution to the surface-mode problem is given by Rayleigh (Ref. 19), and Landau and Lifshitz (Ref. 17 ), for example. By integration of Eq. 13 with this solution it was found that, for the lowest mode:

$$\dot{E} = \frac{31 \pi D_s^3 A^2}{60} \quad (16)$$

The lowest resonant frequency is given by

$$\omega^2 = \frac{64 \sigma}{\rho_l D_s^3} \quad (17)$$

#### DISSIPATION BY PERIODIC DROPLET SHATTERING

If droplets are shattered in a periodic manner, acoustic energy can be converted to surface energy of the drops. The increase in energy is



ROCKETDYNE • A DIVISION OF NORTH AMERICAN AVIATION, INC

proportional to the increase in surface area. Assuming a droplet to be broken into several equally sized droplets, the energy increase is

$$\Delta E = \sigma \pi D_s^2 (n^{2/3} - 1) \quad (18)$$

where  $n$  is the number of droplets formed from the initial droplet. The difficulty that arises in this case is in estimating the frequency of shattering.

Various studies of droplet shattering have been made (Ref. 35 through 37). In these studies the interest was the behavior of drops exposed to open velocity fields, e.g., the flow field following a shock wave. Unfortunately, this is a different situation from that encountered by a droplet located on a surface. These studies have shown, however, that the principal source of breakup is associated with the relative velocity between the gas and droplet, rather than impulsive-pressure forces. This indicates that shattering of a drop on a surface will not be important unless it is exposed to a tangential velocity. It is likely that the drops will be swept from the surface before shattering occurs under these circumstances. The drop removal will involve an energy exchange, in the form of surface energy and kinetic energy, but this is a considerably less dissipative effect than shattering a droplet into several "sub-droplets." Because shattering studies indicate no means of estimating the number of drops formed from a single drop or the frequency of drop shattering, the comparison in a subsequent section is made with assumed values for these parameters.



ROCKETDYNE • A DIVISION OF NORTH AMERICAN AVIATION, INC

## EFFECTS OF ALUMINUM ON COMBUSTION INTERACTION OF THE BURNING SURFACE

It seems possible that agglomerates of aluminum on the burning surface could physically block interaction with the acoustic field. However, the time-average burning rate of solid propellants is not greatly affected by the addition of aluminum. This suggests that, on the average, the non-aluminum portion of the propellant burns about the same as a non-aluminized propellant. From this it appears unlikely that one can even crudely estimate the effect of aluminum in this case. Such estimates must await analysis of the heterogenous combustion problem involving the aluminum. This is an exceedingly complex problem, and appears totally intractable.

In the same category fall those effects caused by the aluminum which involve disturbance of the energy feedback to the surface. If the role played by these effects in combustion instability is to be determined it must be done through careful experimentation, allowing delineation of their influence. The measurement of surface and chamber-volume effects which constituted the experimental part of this program, allows an estimate of these influences to be made.

### Comparison of Damping Mechanisms

To compare particulate damping, the principal volumetric effect associated with the presence of the aluminum, with aluminum effects on or near the burning surface, it is necessary to weight each contribution by the number of droplets of each type. Therefore, the number of droplets in the main volume relative to the number on the surface must be estimated.



ROCKETDYNE • A DIVISION OF NORTH AMERICAN AVIATION, INC

Photographs of the burning surface of heavily aluminized propellants have shown the surface to be nearly covered with molten aluminum, at least at times. To approximate this situation, the surface was assumed to be covered by spheres which touched each other and whose line of centers formed a square pattern. The number of drops on such a surface is given by

$$N_s = \frac{4 S_b}{\pi D_s^2} \quad (19)$$

The number of droplets suspended in the gas phase can be obtained from the mass ratio,  $C_m$ , assuming its value to be known. From the definition of  $C_m$ , the number of droplets is found to be

$$N_v = \frac{6 C_m \delta V}{\pi D_v^3} \quad (20)$$

The value of  $C_m$  was calculated by assuming all of the aluminum to be oxidizer to  $Al_2O_3$ .

For a motor with a cylindrical perforation and burning radially, the ratio of numbers of drops is found to be

$$\frac{N_v}{N_s} = \frac{3}{8} \frac{D_s^2 D C_m \delta}{D_v^3} \quad (21)$$

For a port diameter of six inches, an aluminum loading of 15 weight percent (or  $C_m = 0.396$ ), and  $\delta = 5.3 (10^{-4})$ , the values shown in Table 1 were calculated.



ROCKETDYNE • A DIVISION OF NORTH AMERICAN AVIATION, INC.

TABLE 1

NUMBER OF DROPS IN GAS VOLUME RELATIVE  
TO NUMBER OF DROPS ON BURNING SURFACE

$D_v$ , microns	$D_s$ , microns	$N_v/N_s$
0.1	100	1.2 ( $10^8$ )
1.0	100	1.2 ( $10^5$ )
10.0	100	1.2 ( $10^2$ )
0.1	1000	1.2 ( $10^{10}$ )
1.0	1000	1.2 ( $10^7$ )
10.0	1000	1.2 ( $10^4$ )

With the values in Table 1, the appropriately weighted contribution from particulate damping was computed. Choosing a pressure amplitude of 10 psi and a frequency of 1000 cps as representative, the values shown in Table 2 were calculated using Eq. 14.

TABLE 2  
WEIGHTED RATE OF ENERGY DISSIPATION  
DUE TO PARTICULATE DAMPING

$D_v$ , micron	$D_s$ , micron	$(N_v/N_s) \dot{E}_{part}$ (ergs/drop-sec)
0.1	100	1.4 ( $10^1$ )
0.1	1000	1.4 ( $10^3$ )
1.0	100	1.4 ( $10^3$ )
1.0	1000	1.4 ( $10^5$ )
10.0	100	1.4 ( $10^5$ )
10.0	1000	1.4 ( $10^7$ )



ROCKETDYNE • A DIVISION OF NORTH AMERICAN AVIATION, INC

This table provides the reference values for other estimates. No attempt has been made to cover a complete range of conditions.

The dissipation rate associated with droplet deformation was estimated by use of Eq. 14. With the following properties:

$$\rho_l c_l \approx \frac{1}{\beta_l} = 7.3 (10^{11}) \text{ dyne/cm}^2$$

$$c_l \approx 5.5 (10^6) \text{ cm/sec}$$

$$\mu_l \approx 2 (10^{-2}) \text{ poise}$$

$$f = 1000 \text{ cps}$$

$$\hat{p} = 10 \text{ psi}$$

the results shown in Table 3 were obtained.

TABLE 3  
RATE OF ENERGY DISSIPATION DUE TO  
DROPLET DEFORMATION

$D_s$ , microns	$\dot{E}$ (erg/drop-sec)
100	$1.2 (10^{-5})$
1000	$1.2 (10^{-4})$

Therefore, droplet deformation appears to be insignificant relative to particulate damping, i.e., Table 2.



ROCKETDYNE • A DIVISION OF NORTH AMERICAN AVIATION, INC

The contribution due to surface modes of oscillation was calculated from Eq. 16. The assumptions made in calculating  $\dot{E}$  for this case were: (1) that resonance is attained by the droplet, (2) that the maximum disturbance of the radius of the drop is 10 percent of its mean value, and (3) the surface tension is 840 dyne/cm (appropriate for aluminum in contact with air at 700 C). At 1000 cps, it was found that  $\dot{E} = 7.3$  erg/drop-sec. The corresponding drop diameter was 830 microns.

Thus, at the chosen conditions, the surface modes are not comparable to particulate damping. They appear to be insignificant, in spite of their relatively greater magnitude with respect to droplet deformation.

It is more difficult to make meaningful estimates in the case of droplet shattering. One can only assume values for the frequency of shattering and the number of new drops formed from an initial drop. If a single, 1000-micron drop is shattered into twenty "sub-droplets," Eq. 18 predicts 175 ergs of energy will be absorbed. The importance of shattering as a dissipation phenomenon then becomes dependent upon the shattering frequency, since the energy associated with the individual shattering event is substantial. As already noted, there is no experimental evidence to draw upon. Thus, shattering at the surface may not occur at all. It is likely that, if it does occur, only a small number of drops, on the average, would shatter during each acoustic oscillation (this number may be fractional).

The dissipation rate for the shattering process is the product of the energy loss per shattering event, the mean number of events per acoustic oscillation, and the acoustic frequency. It is clear from the discussion that the lower limit is negligibly small. Under optimum conditions for this process, however, it may compare favorably with particulate damping



ROCKETDYNE • A DIVISION OF NORTH AMERICAN AVIATION, INC

as a dissipation factor. (It must be borne in mind that other factors, not at all understood at present, also enter into overall consideration of the droplet shattering mechanism. For example, what further role, if any, is played by droplets resulting from the shattering of a surface drop. Also, after shattering occurs does reformation through coalescence occur to a significant extent).

The analysis presented indicates that particulate damping is, in general, the dominant dissipation mechanism in the high frequency range, and for the processes considered. It is possible, however, that the effects of the aluminum on combustion interaction with the acoustic field are important to stability. A similar statement may be made concerning droplet shattering. These dissipation mechanisms must be accepted as insufficiently accessible to analysis of the desired precision, so that further success with this problem is possible only through experiment. The results of the experimental portion of this program suggest that these surface effects may indeed play a role in characterizing the "stability" of a propellant, although a role subordinate to that of particulate damping.

Before considering the experimental phase of the program, a brief digression will be made to consider a portion of the analysis which was devoted to nonacoustic instability.

#### THE EFFECTS OF ALUMINUM ON NONACOUSTIC INSTABILITY

Nonacoustic instability has been studied rather extensively (Ref. 1, 20, 22, and 28). These studies suggest that the inclusion of powdered aluminum may be a destabilizing influence, i.e., the aluminum has a detrimental effect on combustion instability. In support of this suggestion



ROCKETDYNE • A DIVISION OF NORTH AMERICAN AVIATION, INC

is the observation that aluminum is shed quasi-periodically from the surface, with a frequency in the range of nonacoustic instability, when burned in the open or in a closed bomb. Therefore, it is of interest to study the effects of aluminum on nonacoustic as well as acoustic instability.

To learn something about these effects, an analytical investigation of nonacoustic instability was carried out. The analysis is described in Appendix B. Several important results were obtained, although most of these are not directly applicable to the effects of aluminum. It was found that the nonacoustic problem could be developed using conventional acoustic methods, the nonacoustic mode being a zeroth-longitudinal acoustic mode for the cavity. This suggested the application of an acoustic-instability combustion model to the nonacoustic case. The Denison-Baum (Ref. 25) model was found to describe the nonacoustic data of Beckstead (Ref. 22) very well. In addition, a detailed comparison between the Denison-Baum model and the acoustic (T-burner) instability data of Horton (Ref. 27) was made. Again, rather good agreement was attained. No previous comparisons of this type have been reported. The combined model was found to explain the "preferred frequency" reported by NOTS (Ref. 28 and 29) and phase-angle data between the oscillatory pressure and light emission, also reported by NOTS (Ref. 29).

With reference to the effects of aluminum, these results suggest two things. First, since the response function (Appendix B) exhibits a maximum in the nonacoustic frequency range, it appears at least possible that the quasi-periodic shedding of aluminum coincides with this maximum. This possibility is arrived at by the following argument: Pressure disturbances generated by the combustion will be reflected back toward the burning surface by the dense cloud of aluminum leaving the surface.



ROCKETDYNE • A DIVISION OF NORTH AMERICAN AVIATION, INC.

Those frequency components of the reflected pressure disturbance which are near the maximum in  $\frac{\mu}{\epsilon}$  will be amplified to a greater extent than others. Thus, lacking an externally imposed frequency, the combustion should tend toward its maximum response, and, presumably, so will the shedding.

The second conclusion of this work is that, if the addition of aluminum has a destabilizing influence, then the influence must be reflected in the  $Re(\frac{\mu}{\epsilon})$ . That is,  $Re(\frac{\mu}{\epsilon})$  for an aluminized propellant must be greater, in the low frequency range, than that for the corresponding nonaluminized propellant.

The experimental results of this program are of interest in this sense. Although the experimental data are not sufficiently precise to warrant firm conclusions, the data consistently indicate that the  $Re(\frac{\mu}{\epsilon})$  is increased by the addition of aluminum. In the high-frequency range, the increase in volumetric damping overwhelms the increase in surface amplification. In the nonacoustic frequency range, however, particulate damping is ineffectual and the apparent increase in  $Re(\frac{\mu}{\epsilon})$  is very important.



## EXPERIMENTAL STUDY

## EXPERIMENTAL APPROACH

It is apparent that an experimental method was needed to measure the effects of aluminum on combustion instability. Accurate data are needed on the volumetric (gas phase) damping and burning-surface response function for highly aluminized propellants and the corresponding non-aluminized propellants. Unfortunately, such data has in the past been inaccessible because of the difficulty in making the appropriate measurements and devising the necessary experiments. The usual T-burner techniques, which are fairly widely used to study acoustic instability of nonmetalized propellants, are not applicable because of the high stability of the metalized system. Merton (Ref. 6) used a conventional T-burner to study the effects of aluminum but he was unable to employ aluminum loadings greater than 1.5 weight percent. Although his study was productive, the aluminum loadings he employed were an order of magnitude too low to be applicable to conventional propellants. A second technique is the shock-tube method (Ref. 30) which has been utilized at Rocketdyne. However, this technique provides no information on particulate damping, apparently the most important damping process. Also, experimental and computational difficulties prevent easy application of the method. The technique which seemed most applicable to obtaining the requisite information was a pulsed T-burner.

Sheng has shown (Ref. 31) that, if a pressure pulse is properly introduced, a T-burner can be used to study propellants too stable to drive oscillations. The pressure pulse must be such that transient pressure oscillations are generated in the T-burner.



ROCKETDYNE • A DIVISION OF NORTH AMERICAN AVIATION, INC

Further, measurements of the rate of decay of these oscillations provide sufficient information to calculate the response function of the burning surface and the volumetric damping. Even though this method suffers from certain limitations it was applied as the best method currently available.

The usual T-burner technique is to measure the growth constant from the rate of oscillatory development at the beginning of a test and the decay constant from the oscillatory decay following burnout (Eq. Ref. 38, 39, and 40). These two kinds of derived data may be interpreted to calculate the response function for the burning surface. The decay constant is taken to represent the overall damping in the system. In a pulsed T-burner, the oscillations do not develop because the damping exceeds the gains. Therefore, after the burning is well established, a pulse is introduced which excites oscillations in the cavity. These oscillations decay because of the excess damping. However, this rate of decay may be interpreted in a manner identical with the usual growth constant. A second pulse is introduced immediately after burnout to measure the overall damping. This damping will include whatever damping is introduced by the pulsing device. Thus, the interpretation of pulsed T-burner data is carried out in a manner essentially identical with conventional T-burner data.

#### EXPERIMENTAL SYSTEM

The T-burner used in this study was similar to that used by other investigators. A sketch of the motor is shown in Fig. 4. The motor was made of steel tubing with dimensions of 1.5-inch ID by 0.5-inch wall thickness (nominally). Interchangeable sections were made so that motor lengths ranging from 41 inches to 9 inches (without propellant) were available. These lengths provided instability frequencies of 200 cps to somewhat more than 2000 cps.



ROCKETDYNE • A DIVISION OF NORTH AMERICAN AVIATION, INC.

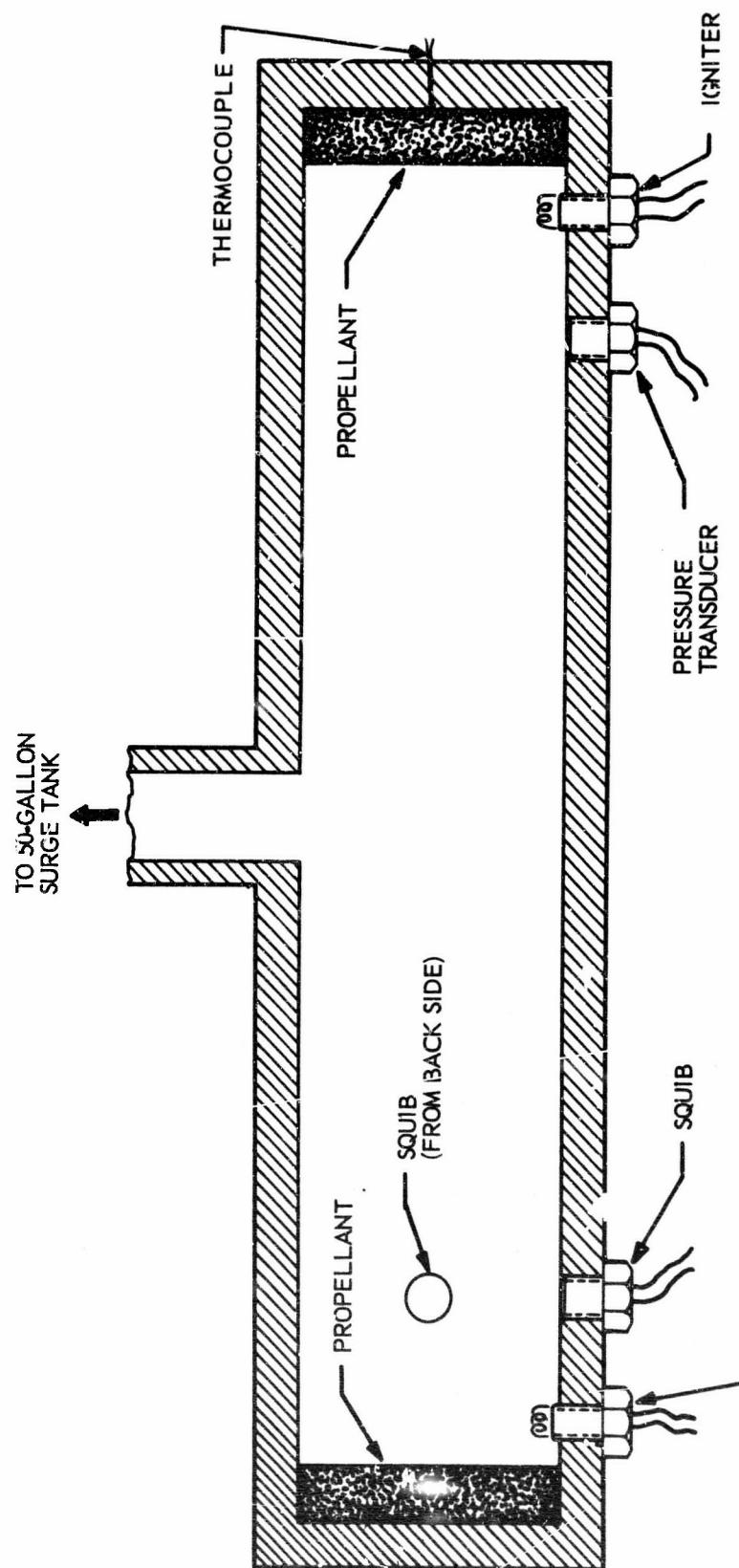


Figure 4. Sketch of the Pulsed T-Burner



ROCKETDYNE • A DIVISION OF NORTH AMERICAN AVIATION, INC

Squibs were used to generate a pressure pulse when necessary. Two squibs were mounted in the curved wall of the motor. For proper pulsing it was necessary to have a positive indication of propellant burnout in the motor. A thermocouple was mounted under one propellant sample to serve this function.

A Kistler pressure transducer (model 603A) was used to measure the oscillatory pressure. Except for the shortest motor, the transducer was mounted in the curved wall of the motor, about 2-3/4 inches from one end. In the shortest motor, the transducer was mounted under the propellant sample in one end closure.

Propellant samples were bonded into each end of the motor with an epoxy adhesive. The propellant was cast into phenolic sleeves (1/16-inch wall thickness) and then cut on a lathe into 1/2-inch lengths. The phenolic sleeves facilitated bonding and prevented burning on the sides of the sample, which can significantly alter results. Lathe cutting provided a uniform and reproducible surface, as well as an accurate length.

Ignition was obtained by burning a small amount of propellant shavings near the propellant surface. The shavings were ignited by burning a 1-1/2-inch (nominal) length of exploding bridge wire (Pyrofuzes). The bridge wire was soldered to the electrical leads of an expended squib (initiator) which eliminated sealing problems and facilitated replacement.

The motor was close-coupled to a 50-gallon surge tank. Before a firing, the surge tank and motor were pre-pressurized with nitrogen. The tank provided good mean-pressure regulation during the test.



ROCKETDYNE • A DIVISION OF NORTH AMERICAN AVIATION, INC

The principal measurement in the system was the pressure. The output of the transducer system (Kistler Model 603A transducer/Kistler Model 504 charge amplifier) was recorded simultaneously by a magnetic tape recorder and by an oscilloscope camera. A secondary measurement was the thermocouple output. This signal was amplified by a Kintel DC amplifier and recorded on magnetic tape and the oscilloscope as well.

The experimental system was operated as follows. The chamber was pressurized to the chosen level. Closing an igniter switch fired the igniters and started an electronic delay generator (thyatron type). This delay circuit fired the first pulse-generating squib about midway through the firing by closing a relay. Near the end of the test, burnout was sensed by the thermocouple. The amplified thermocouple output triggered a second electronic delay generator which fired the second squib about 90 milliseconds after the equilibrium thermocouple output was reached.

Three kinds of squibs were used in this program. New squibs would have been prohibitively expensive; however, several kinds of squibs were available from supply at no cost. The first two kinds were used until the available supply was exhausted. Through test 40, a Rocketdyne initiator designated as NA5-26523-1A was used, when applicable. For tests 41 through 140, a Holex Corp. squib with Holex designation of 2374 was used, when applicable. For tests 141 through 183, a second Holex squib designated as 1785 was used. All three squibs were able to excite oscillations in the motor. The first squib was rather unsatisfactory because it introduced excessive damping, apparently due to condensed-phase combustion products. The latter two were satisfactory in this regard and seemed to be equivalent for purposes of this experiment.



ROCKETDYNE • A DIVISION OF NORTH AMERICAN AVIATION, INC

Several CTPB/AP-type propellants were used in this study. They are tabulated in Table 4. Aluminum content was varied with the proportions of other constituents remaining constant. The aluminum was Valley Metallurgical H-30 with a mass-mean diameter of  $35 \mu$  according to micrograph analysis. Composition of these propellants was chosen to cover an adequate range of aluminum loadings and to be similar to propellants which have been studied extensively by other investigators.

TABLE 4  
COMPOSITION OF PROPELLANTS USED

Propellant	Composition (weight percent)				
	A	B	C	D	E
Binder	20	19	17	20	19
Fine AP ( $20 \mu$ , nominal)	39	37	33.2	40	38
Coarse AP ( $150 \mu$ , nominal)	39	37	33.2	40	38
Copper Chromite	2	1.9	1.7	0	0
Aluminum	0	5	15	0	5



ROCKETDYNE • A DIVISION OF NORTH AMERICAN AVIATION INC

## EXPERIMENTAL RESULTS

The experimental pressure data were interpreted in terms of a growth constant,  $\alpha$ , where  $\alpha$  is defined by the time dependence of the data. This dependence, as long as the amplitude is not too large, is given by  $e^{\alpha t} \cos \omega t$ . At high amplitudes,  $\alpha$  is no longer constant and becomes dependent on the amplitude. If the oscillations decay,  $\alpha$  is negative. Growth constants were calculated from the pressure data by plotting the double-amplitude (peak-to-peak) against time on semilogarithmic coordinators. On such a plot, the slope of the data represents  $\alpha$ . The double-amplitude was measured from oscillograph traces made, at reduced speed, from the originally recorded data. A smooth curve was drawn through the oscillatory peaks and this was taken to represent the amplitude at each time increment.

For the most part, the data were well represented by the exponential type of time dependence, even for those runs in which the oscillations decayed very rapidly. In some of the low-frequency tests, the waveform contained significant harmonic distortion. The data from these runs were closely low-pass filtered to minimize the harmonic content. Scatter in the completed values of  $\alpha$  increased with frequency, undoubtedly much of this can be associated with the very high decay rates encountered in this region.

The observed value of  $\alpha$  is the sum of several contributions (Ref. 26). Individual contributions can be evaluated by appropriate subtraction of the  $\alpha$ 's which are measured in different kinds of measurements. Such an approach is used to evaluate the real part of the response function,  $\text{Re} \left( \frac{\mu}{\epsilon} \right)$ , from the growth constant measurements. The relationship is (see, for example, Ref. 38, 39):

$$\text{Re} \left( \frac{\mu}{\epsilon} \right) = \frac{p_0}{r\rho_s} \frac{L}{2c^2} (\alpha_b - \alpha_{nb}) \quad (22)$$



ROCKETDYNE • A DIVISION OF NORTH AMERICAN AVIATION, INC.

In Eq. 22 the assumptions were made that (1)  $\alpha_b$  is the sum of a contribution from the burning surface and the contributions from all the damping processes, and (2) that  $\alpha_{nb}$  represents all of the damping contributions.

The additive character of the  $\alpha$ 's can be used to obtain the attenuation coefficient for the increase in volumetric damping due to the aluminum. This damping is thought to be essentially entirely due to particulate damping. The quantity  $\alpha_{nb}$  is the sum of a contribution due to the presence of aluminum and a contribution from other damping processes. The  $\alpha$  from these "other damping processes" was assumed equal to the  $\alpha_{nb}$  obtained from a squib test with no aluminum present. Through these assumptions the growth-constant data were evaluated to determine the changes in response function and volumetric damping for the aluminized propellants relative to the non-aluminized propellants.

Tests were made at mean-pressure levels of 200, 400, and 600 psi with motor lengths of 9, 15, 21, and 41 inches and with propellants A, B, C, D, and E (Table IV). To thoroughly determine the growth constants for each of these conditions, a prohibitively large number of tests would be required. Because of this, emphasis was placed on propellants A and C and pressure levels of 200 and 600 psi with all motor lengths. Fewer tests were made at the other conditions, however, the results of these tests are entirely commensurate with those of the more thoroughly studied conditions. In addition to the propellant tests, a number of tests were made with only the igniter and one squib being fired. These tests were made to evaluate the damping introduced by the squib, the igniter being burned to heat the gas in the motor before pulsing. The growth constants obtained from all tests are tabulated in Appendix C. Most of the data are plotted in Fig. 5 through 18.



ROCKETDYNE • A DIVISION OF NORTH AMERICAN AVIATION INC

On Fig. 5 are plotted the growth constants obtained from a propellant at 200 psi. In this case the motor is unstable and oscillates throughout the tests; therefore,  $\alpha_b$  is a positive number. The curves through the data were used to evaluate  $Re(\frac{\mu}{\epsilon})$  for this propellant. On Fig. 6 are shown similar values for C propellant at 200 psi. The solid curves were drawn to represent the data. In this case, the motor is stable and pulsing was necessary. Therefore, the plotted values include a damping contribution from the squib. These curves may be used to calculate  $Re(\frac{\mu}{\epsilon})$  for this propellant. Note that in Eq. 22 the coefficient of the term  $(\alpha_b - \alpha_{nb})$  is approximately the same for each propellant since the burning rates appear equal from the data. If the  $Re(\frac{\mu}{\epsilon})$  was unaltered by the presence of aluminum, as found by Horton (Ref. 6) with lightly aluminized propellants, the vertical distance between the solid curves on this plot would equal the difference in growth constants for A propellant shown on Fig. 5. This difference from Fig. 5 has been added to the  $\alpha_b$  curve on Fig. 6 and is shown as the dashed curve. The dashed curve is the  $\alpha_{nb}$  curve that would be obtained if  $Re(\frac{\mu}{\epsilon})$  were the same as that for A propellant.

The data indicate that the  $Re(\frac{\mu}{\epsilon})$  is approximately doubled by the addition of aluminum. The indication that the aluminum destabilizes the burning surface is an important consideration which appears in all of the experimental results. Refinement of the experimental technique should be carried out to eliminate all possibility of systematic errors and to further verify this apparent amplification.

If the surface has been greatly stabilized by the aluminum, the difference in growth constants would have been negative, i.e., the  $\alpha_{nb}$  curve would have been below the  $\alpha_b$  curve. Clearly, within the limitations of the



ROCKETDYNE • A DIVISION OF NORTH AMERICAN AVIATION, INC

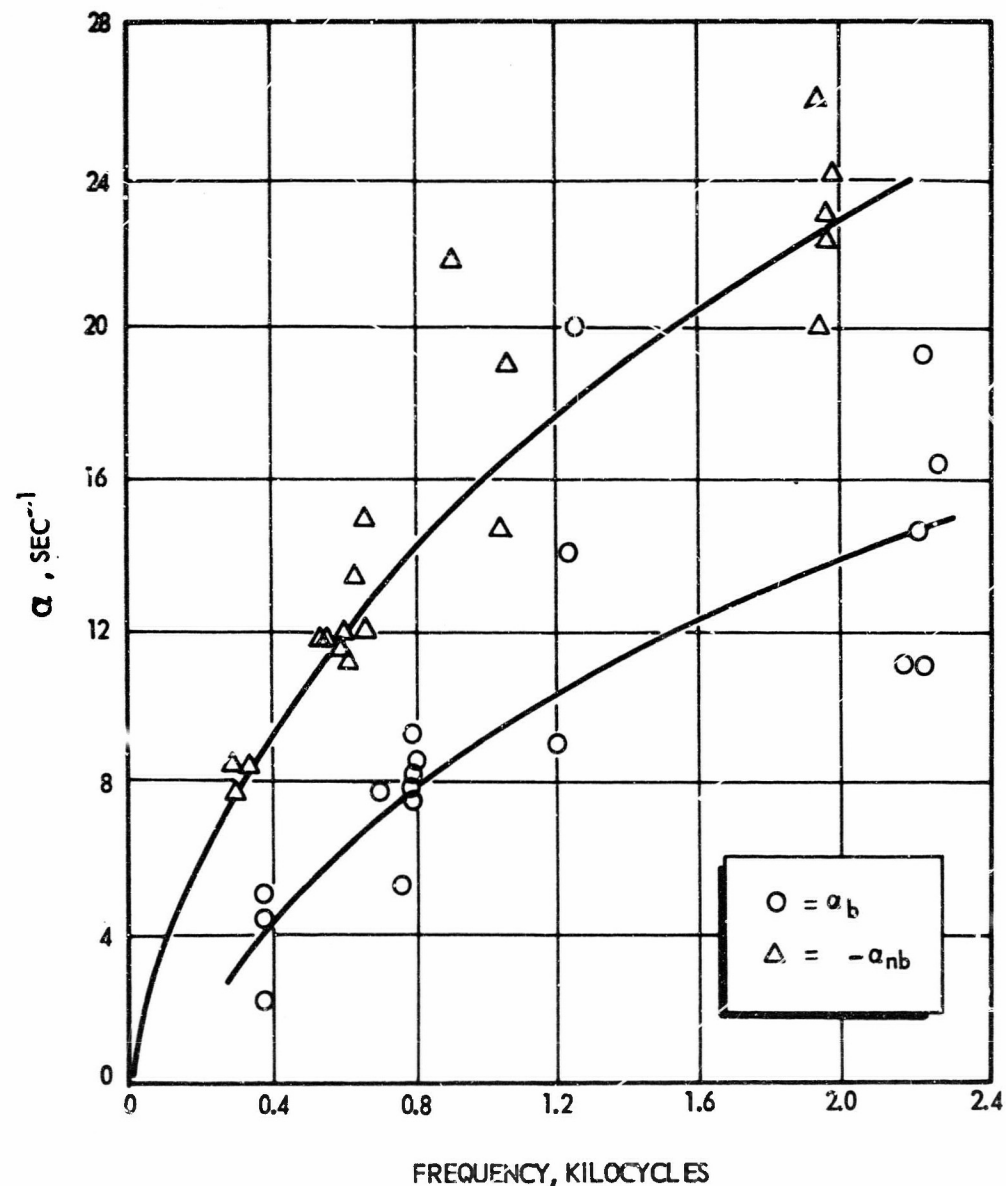


Figure 5 . Decay-Rate Data for A-Propellant at 200 psi



ROCKETDYNE • A DIVISION OF NORTH AMERICAN AVIATION, INC.

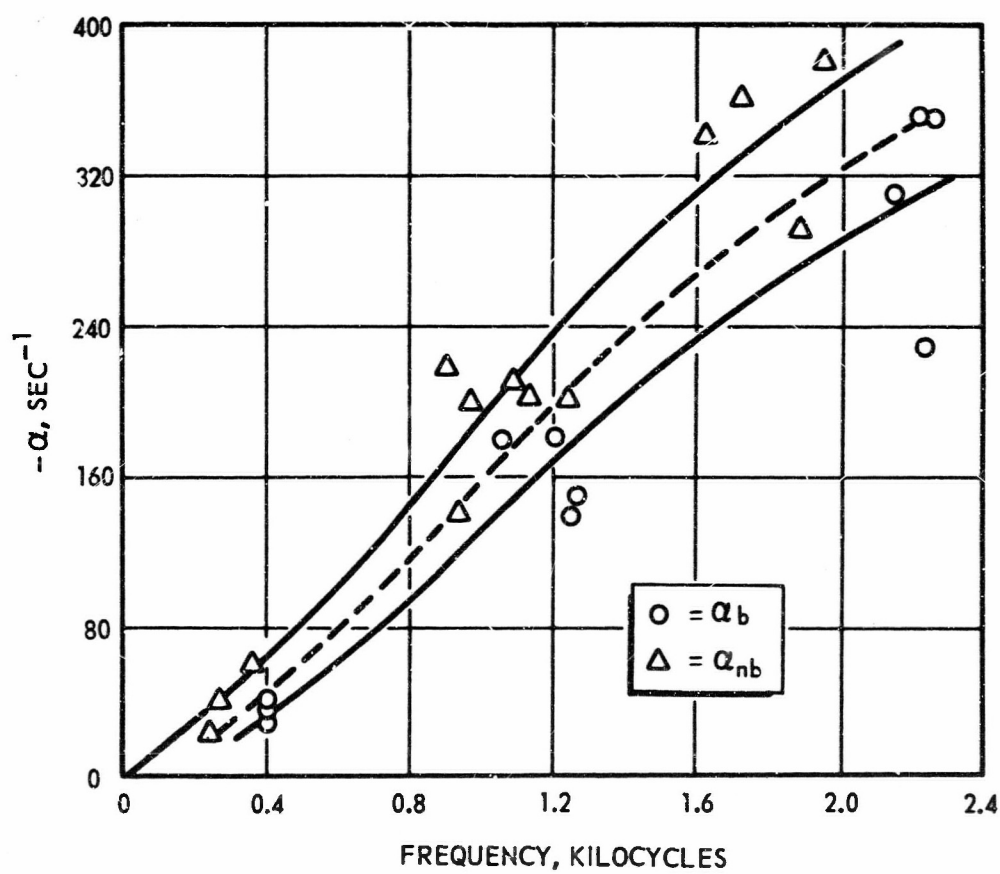


Figure 6. Decay-Rate Data for C-Propellant at 200 psi



ROCKETDYNE • A DIVISION OF NORTH AMERICAN AVIATION INC

data, the surface is not stabilized by the aluminum. Also it is clear that increased overall stability of aluminized propellants must be due to increased volumetric damping. It is likely that the increased volumetric damping is principally particulate damping.

The increase in volumetric damping due to the aluminum was calculated as follows. The damping associated with the motor and squib was evaluated from the tests with only a squib and igniter being fired. These data are shown in Fig. 7. At the two higher pressures the  $\alpha_{nb}$  data from the A propellant tests were also used. All of these data are described by a similar curve (Fig. 11 and 14) so that these additional data provide some support for the extrapolation to higher frequencies shown in Fig. 7. The particulate damping was calculated from the  $\alpha_{nb}$  data by subtracting the extraneous contribution defined by the curve on Fig. 7. These calculated points are shown on Fig. 8. It is apparent that the particulate damping was substantial.

Also shown on Fig. 8 are two curves. These curves were calculated from particulate-damping theory (either the Temkin or Epstein-Carhart model) for the indicated mean particle size. The important observation here is that a fixed mean-particle size will not describe the data from the several motors. The data fall in the region where the  $D_{53}$  mean size is appropriate. The data indicate that the size distribution changes with the length of the motor. Morton (Ref. 7) also considered a change in particle size to be likely.

The results from A and C propellants at 600 psi were much the same as those just discussed. On Fig. 9 are shown the growth constants obtained from A propellant. In this case the motor was stable and pulsing was



ROCKETDYNE • A DIVISION OF NORTH AMERICAN AVIATION, INC

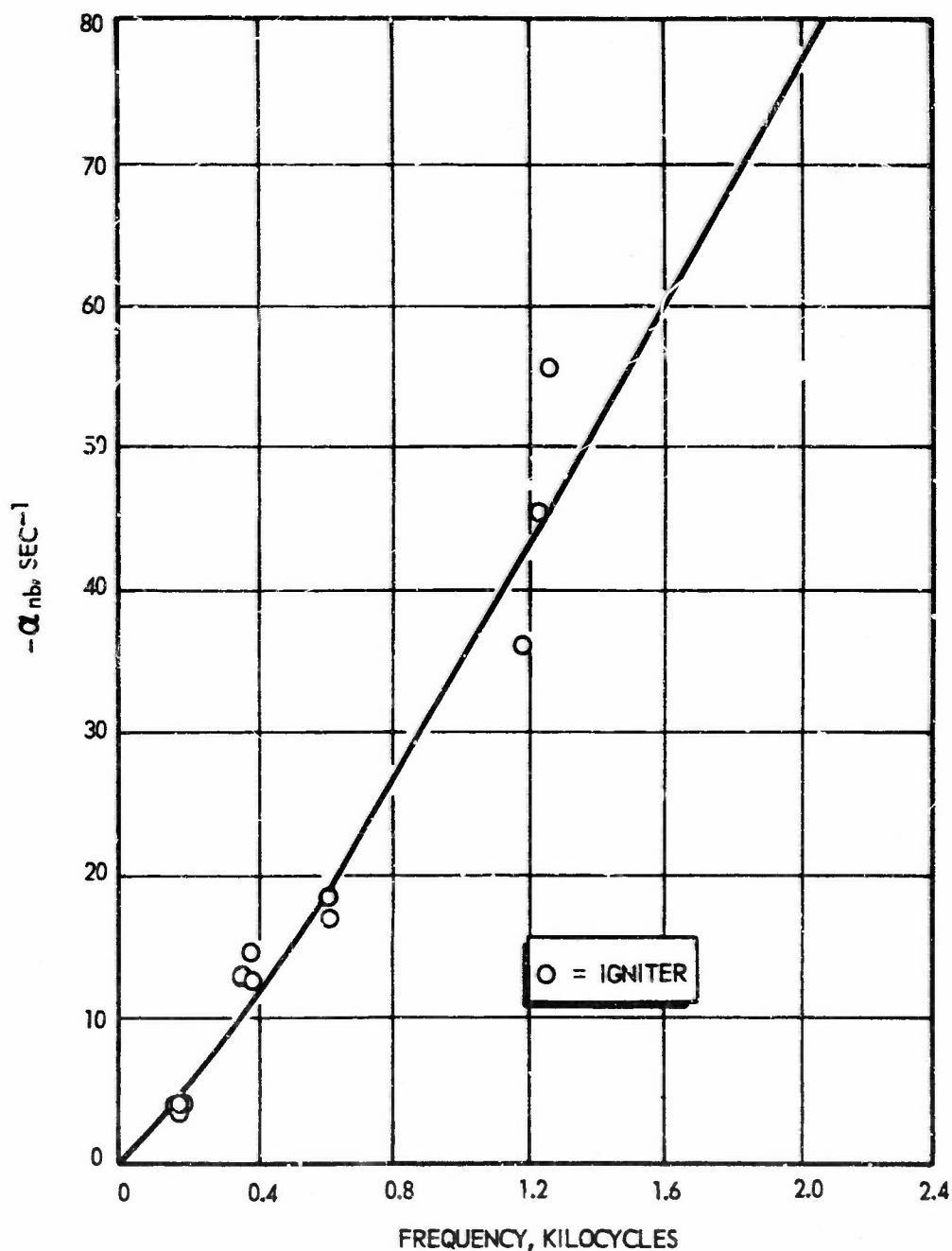


Figure 7 . Decay-Rate Data for P-4 Squibs at 200 psi



ROCKETDYNE • A DIVISION OF NORTH AMERICAN AVIATION, INC.

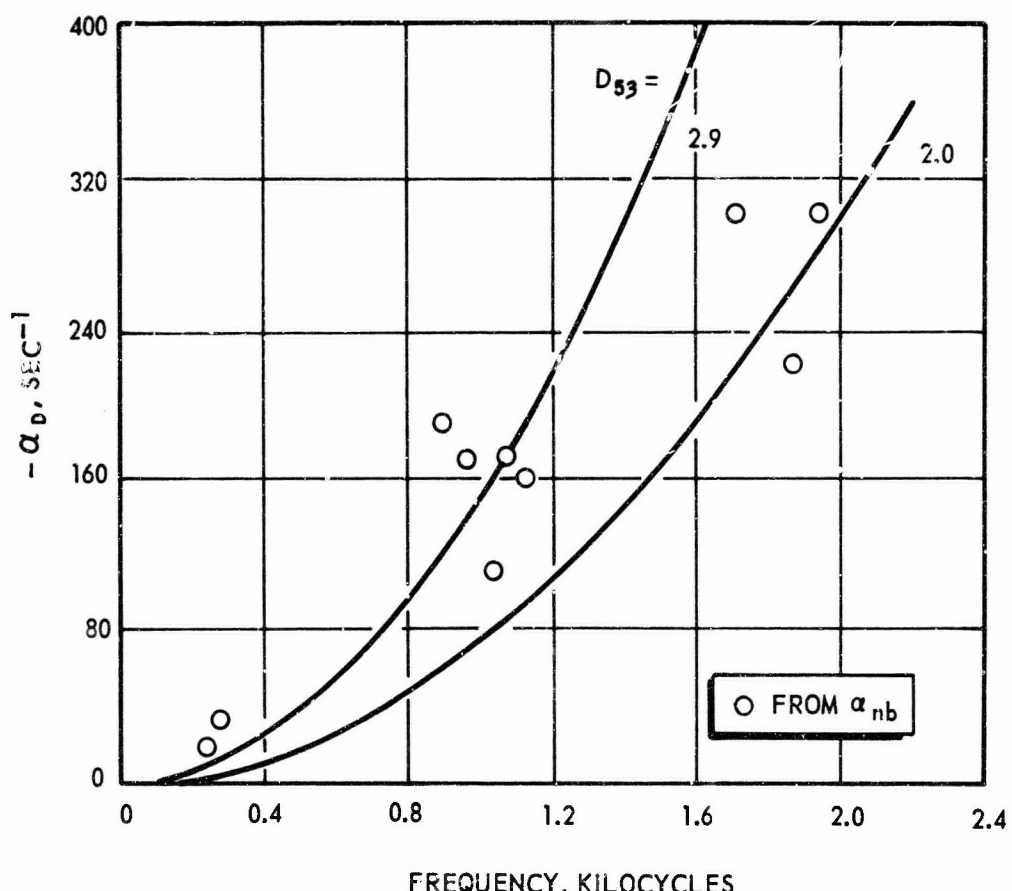


Figure 8 . Comparison of Experimentally Determined Particulate Damping With Constant Particle-Size Curves for C-Propellant at 200°C



ROCKETDYNE • A DIVISION OF NORTH AMERICAN AVIATION, INC.

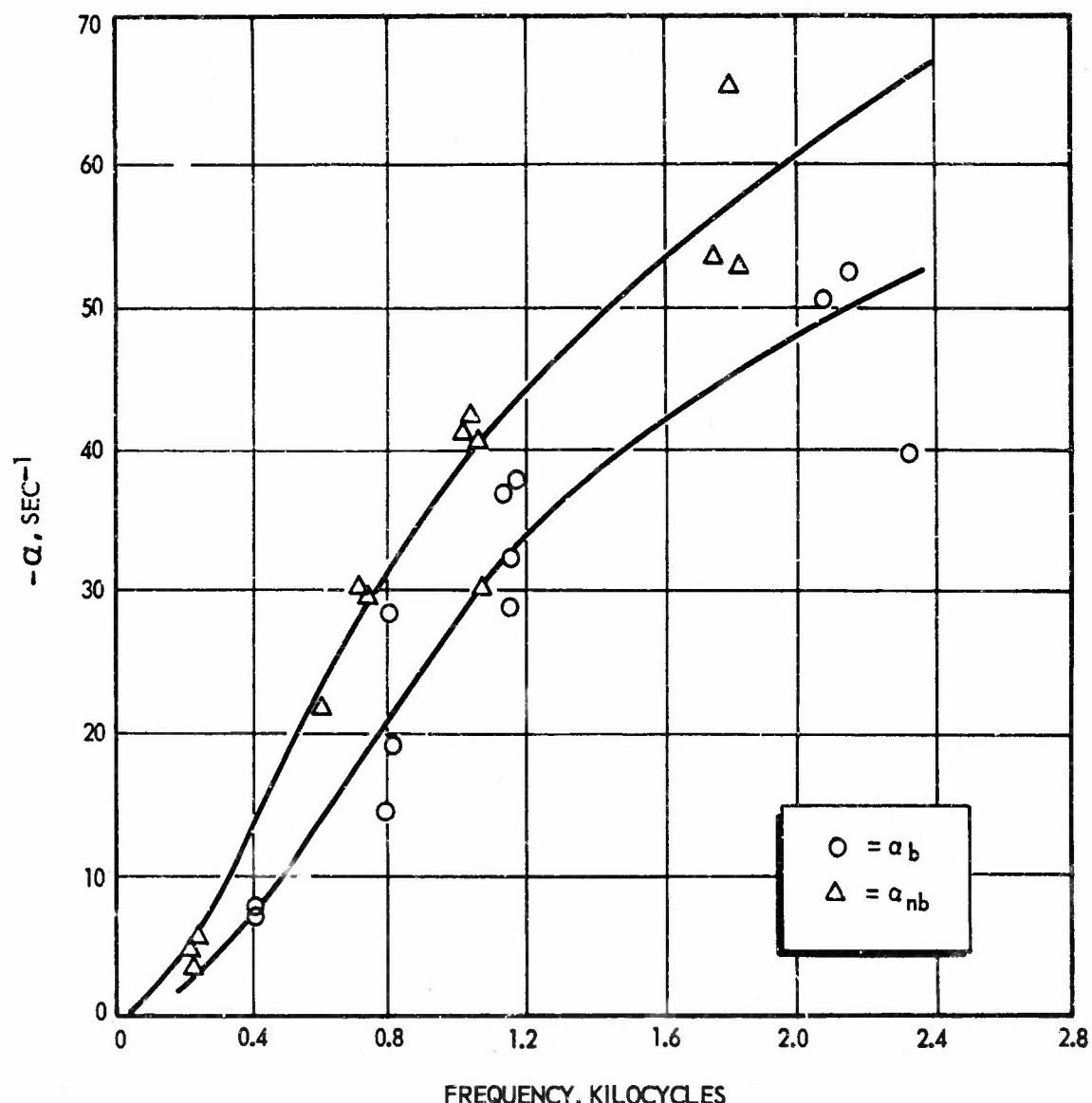


Figure 9 . Decay-Rate Data for A-Propellant at 600 psi



necessary. Figure 10 shows the corresponding results for C propellant. On this plot the dashed curve again represents the  $\alpha_{nb}$  curve that would be obtained if the  $Re(\frac{H}{\epsilon})$  were the same as for A propellant. Clearly, the results indicate the aluminum greatly increases  $Re(\frac{H}{\epsilon})$ , even more so than at 200 psi. The damping attributed to the motor and squib is shown in Fig. 11.

The results of the particulate-damping calculations are shown on Fig. 12. On this plot, the circles were obtained in the same manner as the values shown on Fig. 8. The second set of points, the triangles, were calculated by assuming the  $Re(\frac{H}{\epsilon})$  to be unchanged by the aluminum, i.e., in the same manner as that used by Horton (Ref. 6). Specifically, the decay rate defined by the  $\alpha_b$  curve for A propellant was subtracted from the  $\alpha_b$  values for C propellant to give the particulate-damping coefficient. Also shown on this plot are three curves calculated from particulate-damping theory. As before, the experimentally determined particulate damping is not described by a single particle-size distribution. Again it is concluded that the size distribution changes with motor length.

Results for A propellant at 400 psi are shown on Fig. 13. The damping attributed to the squib and motor is shown on Fig. 14. The results obtained from B propellant at 200, 400, and 600 psi are shown on Fig. 15, 16, and 17, respectively. All of these results are very similar to those discussed previously. Further growth constant data, which have not been plotted, are tabulated in Appendix C. These data compare well with those that have been plotted.

Some additional observations concerning particulate damping may be made. Experimentally, the effects of pressure on particulate damping appear small, as is indicated by a comparison of Fig. 8 and 12. Particulate



ROCKETDYNE • A DIVISION OF NORTH AMERICAN AVIATION, INC.

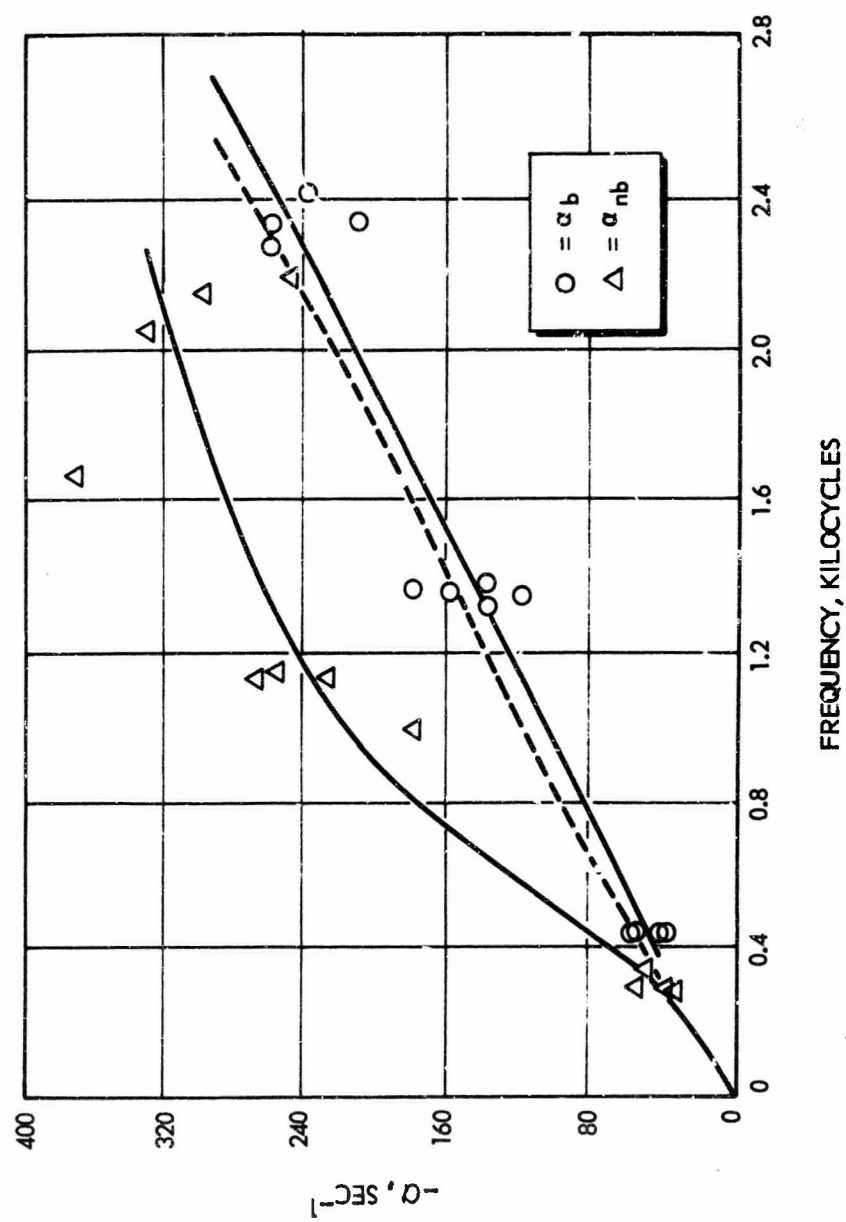


Figure 10. Decay-Rate Data for C-Propellant at 600 psi



ROCKETDYNE • A DIVISION OF NORTH AMERICAN AVIATION INC

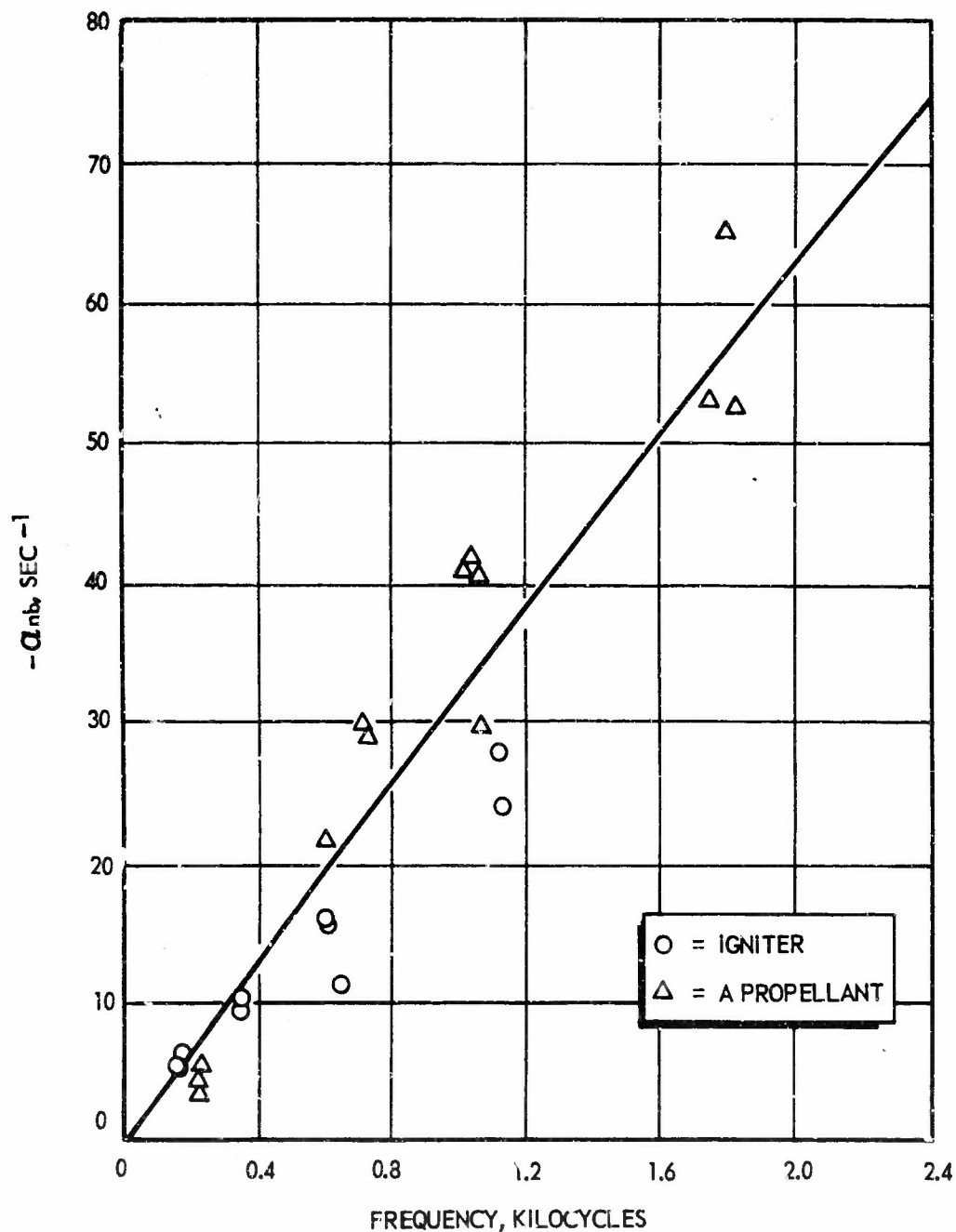


Figure 11. Decay-Rate Data for P-4 Equibs at 600 psi



ROCKETDYNE • A DIVISION OF NORTH AMERICAN AVIATION, INC

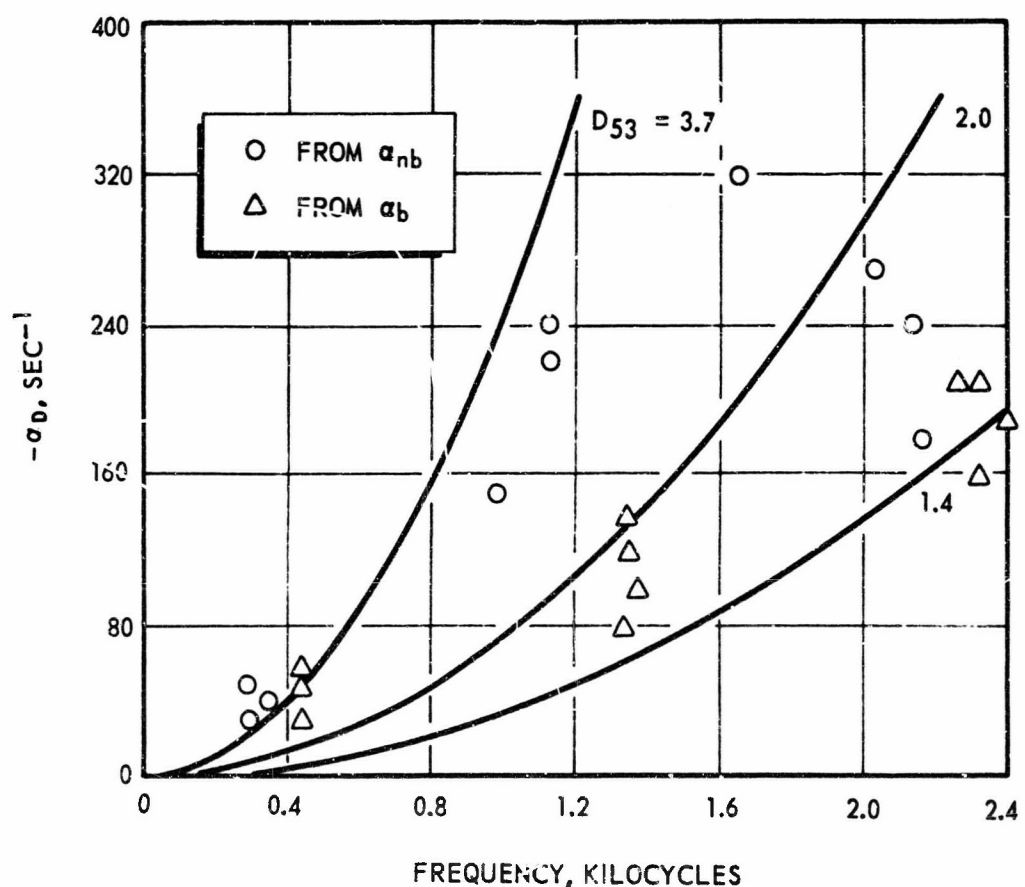


Figure 12. Comparison of Experimentally Determined Particulate Damping With Constant Particle-Size Curves for C-Propellant at 600°C



ROCKETDYNE • A DIVISION OF NORTH AMERICAN AVIATION INC

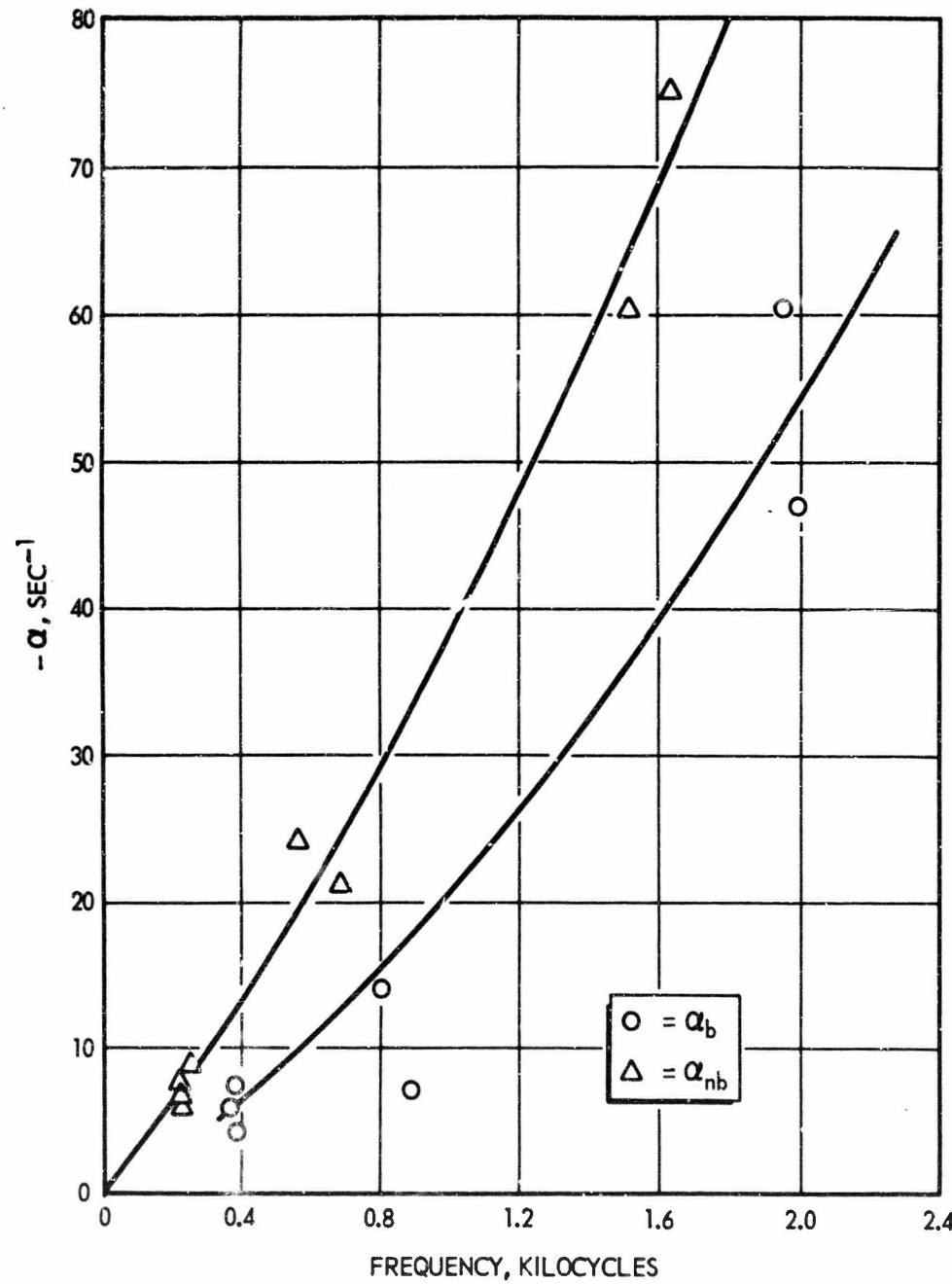


Figure 15. Decay-Rate Data for A-Propellant at 400 psi



ROCKETDYNE • A DIVISION OF NORTH AMERICAN AVIATION INC

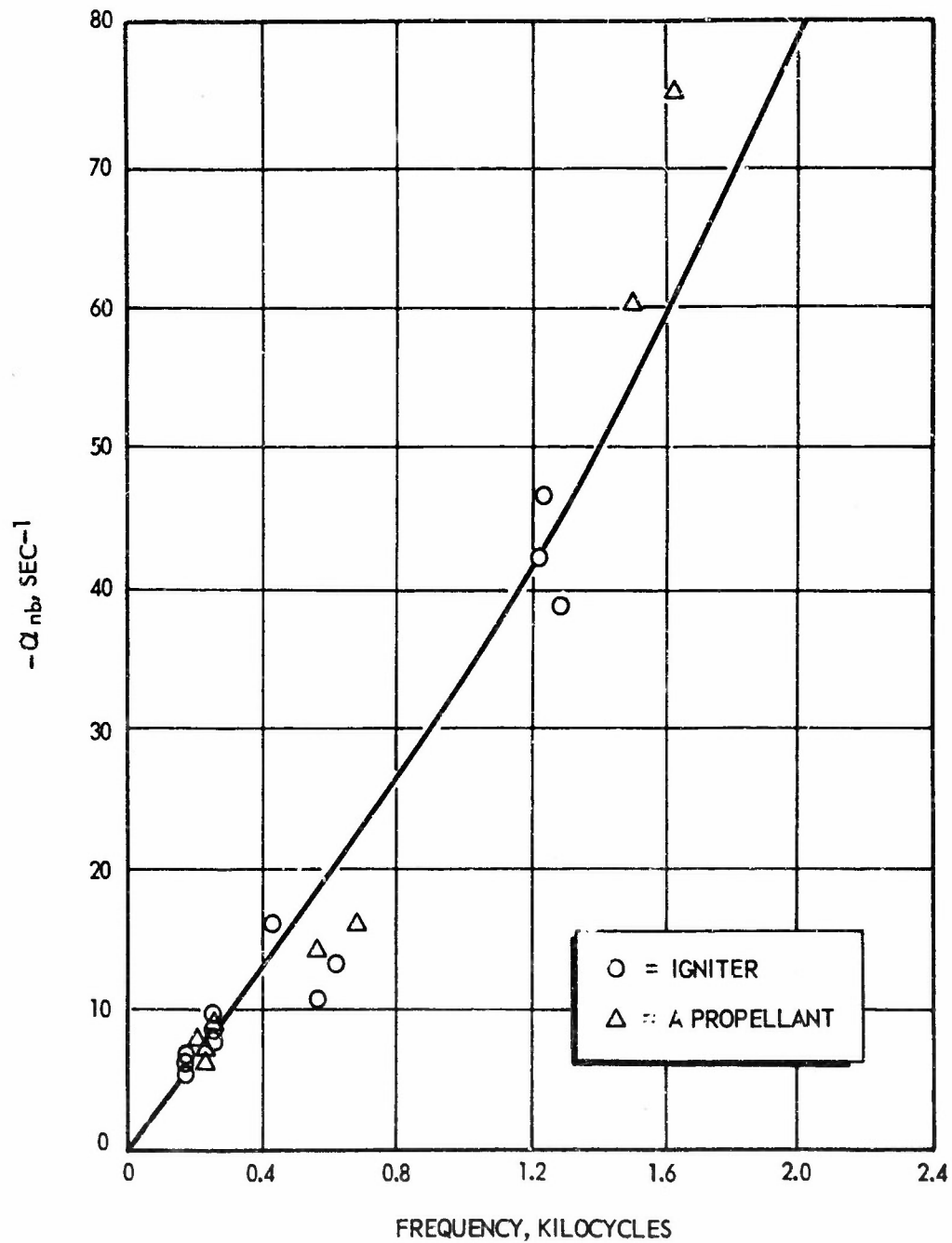


Figure 14. Decay-Rate Data for P-4 Squibs at 400 psi



ROCKETDYNE • A DIVISION OF NORTH AMERICAN AVIATION INC

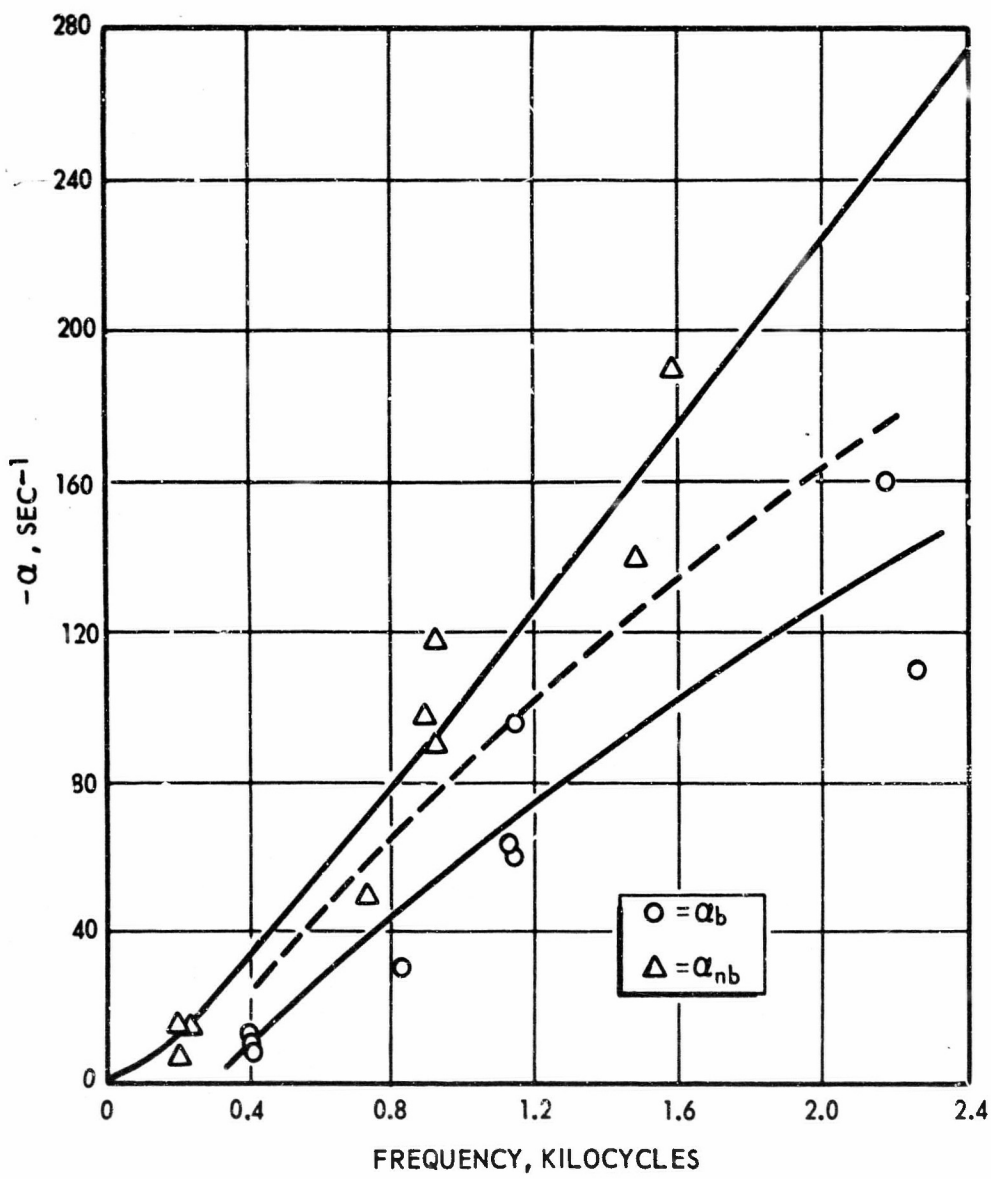


Figure 15. Decay-Rate Data for B-Propellant at 200 psi



ROCKETDYNE • A DIVISION OF NORTH AMERICAN AVIATION, INC

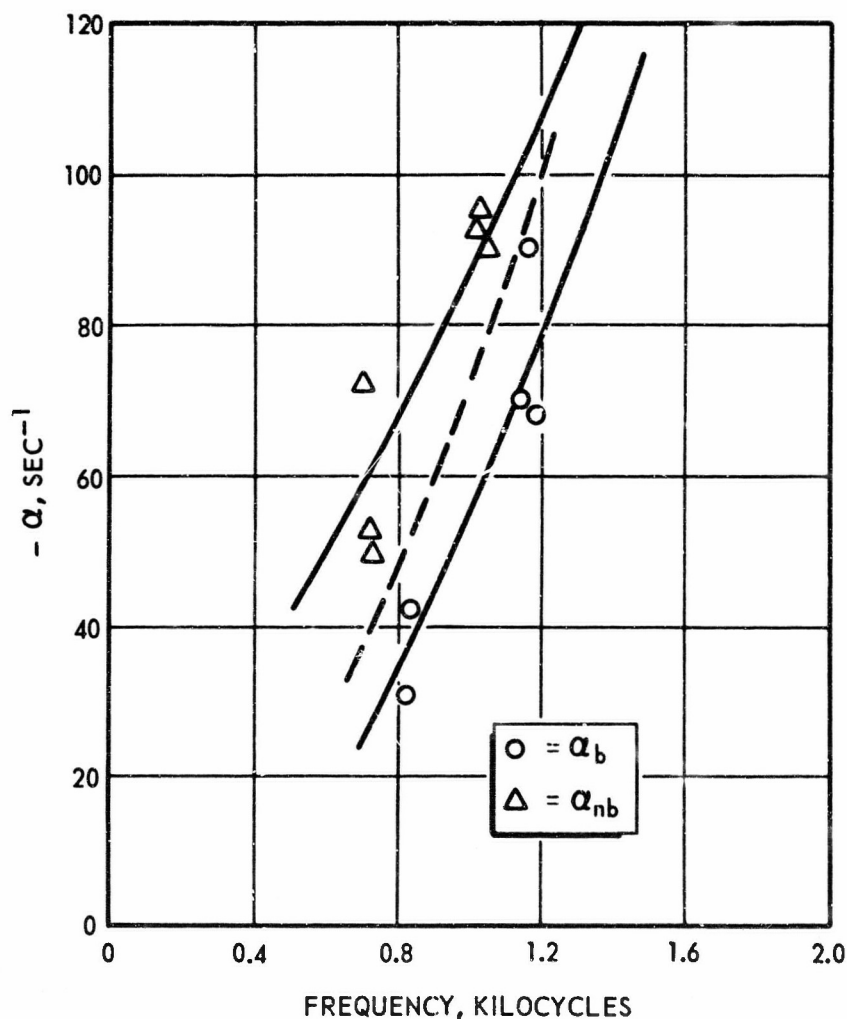


Figure 16 . Decay-Rate Data for B-Propellant at 400 psi



ROCKETDYNE • A DIVISION OF NORTH AMERICAN AVIATION, INC.

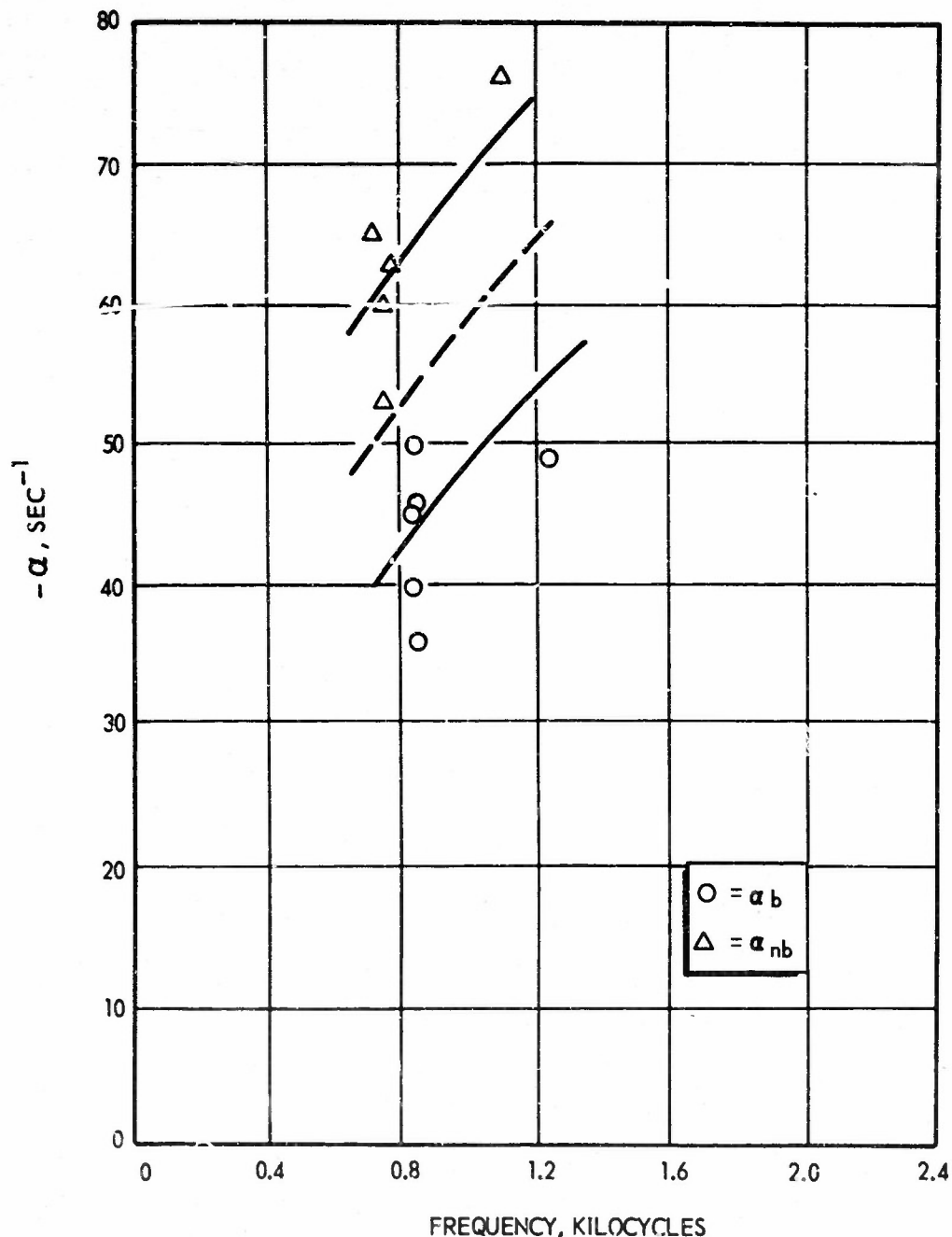


Figure 17. Decay-Rate Data for R-propellant at 600 psi



ROCKETDYNE • A DIVISION OF NORTH AMERICAN AVIATION INC

damping theory predicts little effect of pressure on damping for a fixed particulate size (Ref. 34). If this is accepted then the experimental results cited indicate the effect of pressure on particulate size to be small.

The effects of particle concentration on particulate damping, as indicated by the experimental results obtained are approximately in accord with theory. On Fig. 18 is shown the experimental dependence of damping on the mass ratio,  $C_m$ . The shape of the curve through the experimental values was calculated according to the Temkin model, Eq. 5. At other frequencies and pressures, comparable results were obtained.

It is evident that the pulsed T-burner employed in these studies, while subject to certain limitations, does provide a powerful tool for investigating the effects which form the subject of this report. In particular, the pulse concept permits the desired separation of surface and chamber volume effects, allowing this to be accomplished at aluminum loadings in the range employed in conventional propellants and inaccessible to conventional T-burner investigation. The results of this separation show that the dominant mechanism by which aluminum operates to promote stability is particulate damping in the gas phase. They further suggest that the aluminum may actually tend to destabilize the burning surface. Although for the motors considered in this report the damping influence outweighs the destabilizing tendency, conceivably in motors possessing a higher ratio of burning surface area to chamber volume the overall stabilizing effect of aluminum could be considerably reduced.



ROCKETDYNE • A DIVISION OF NORTH AMERICAN AVIATION, INC.

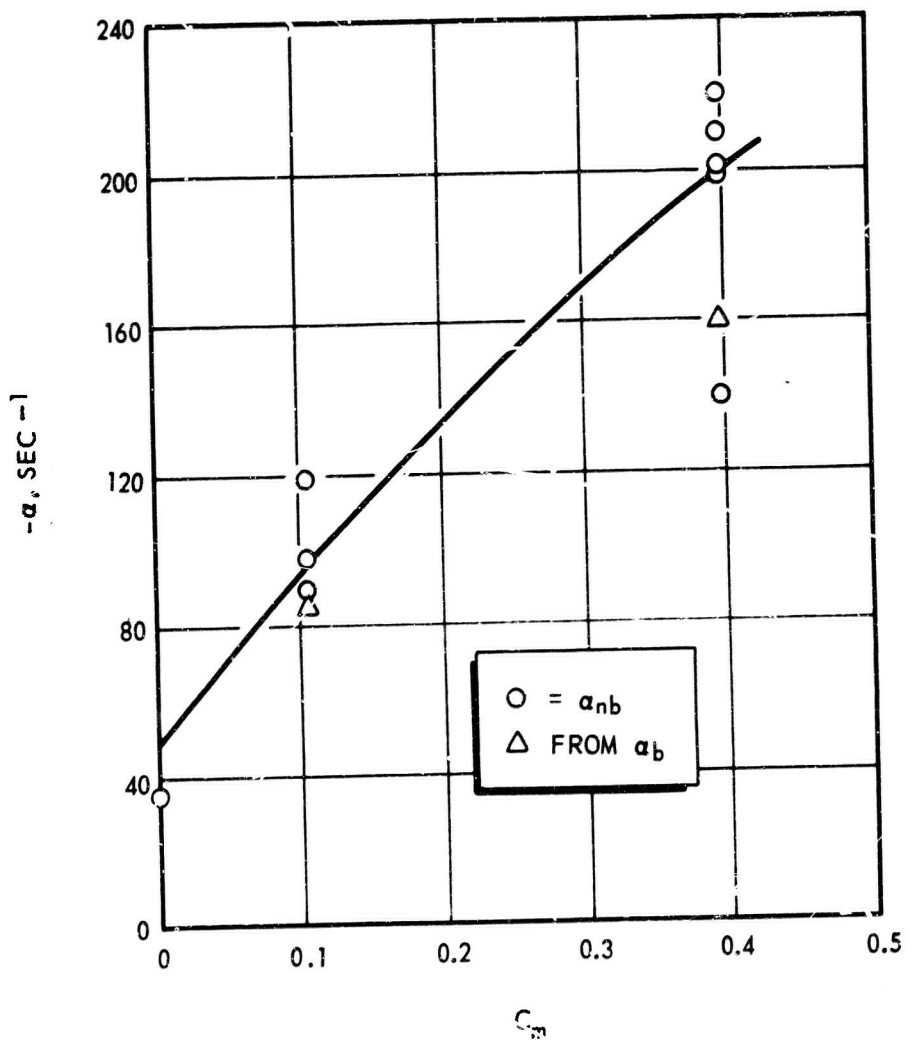


Figure 18. Experimental Concentration Dependence of the Particulate Damping for B-and C-Propellants at 200 psi and 1000 cps



ROCKETDYNE • A DIVISION OF NORTH AMERICAN AVIATION, INC.

### CONCLUSIONS AND RECOMMENDATIONS

The investigation reported has been considerable success in throwing light upon the role of aluminum in combustion instability of solid propellants. This effort represents the first successful attempt to obtain quantitative information on the stability characteristics of propellants which contain sufficient aluminum to be of practical interest. Further, the broad scope of the program has been fruitful in developing interesting areas for further research.

The analytical phase has indicated that:

1. The dominant stabilizing influence associated with aluminum is due to particulate damping in the chamber volume.
2. Various kinds of oscillatory motion of the droplet are not likely to play an important role.
3. Drop shattering is probably unimportant unless the shattering frequency is greater than one would reasonably estimate. Photographic studies are needed to determine the extent of shattering.
4. The effect of aluminum in modifying the interaction between the acoustic field and the combustion may be significant (though probably still small with respect to particulate damping). However, analysis of this interaction was found to be completely intractable, since it would require analysis of the complete heterogeneous combustion problem.
5. Nonacoustic instability is closely related to acoustic instability. This relationship suggests the need to apply the current knowledge of the latter to improve understanding of the former.



ROCKETDYNE • A DIVISION OF NORTH AMERICAN AVIATION, INC.

6. The Denison-Baum combustion model can be used to quantitatively describe both acoustic and nonacoustic instability data. The nonacoustic instability data included data from 10 percent aluminized propellants. Further use of this model to explain experimental observations is suggested.
7. Quasi-periodic shedding of droplets from the burning surface is likely to occur with a frequency near the maximum in the response function curve. Experimental consideration of this relationship is needed.

During the experimental study, instability data were obtained from propellants containing up to 15 weight percent aluminum and at pressure levels as high as 600 psi. Although the data are of limited precision, important information was obtained. The data indicate that:

1. Particulate damping is the dominant mechanism whereby aluminum stabilizes acoustic instability at all aluminum loadings. Substantial particulate damping was found, being measurable at frequencies as low as 200 cps.
2. The inclusion of aluminum destabilizes the burning surface over the entire frequency range; i.e., the surface has increased ability to amplify a pressure disturbance.
3. The particle-size distribution varies with T-burner length.
4. The pressure effect on particulate damping is small, which implies that the pressure dependence of the particle-size distribution is small.
5. The effect of aluminum concentration is reasonably in accord with theory.



ROCKETDYNE • A DIVISION OF NORTH AMERICAN AVIATION, INC

Further, more precise experimental work is needed to fully verify each of these indications. The destabilization of the burning surface is particularly important, both for acoustic and nonacoustic instability.

Finally, the experimental study has demonstrated the effectiveness of a pulsed T-burner as a means of studying propellants too stable to drive the T-burner.

## REFERENCES

1. Price, E. W., "Experimental Solid Combustion Instability," Tenth Symposium (International) on Combustion, Combustion Institute, Pittsburgh, Pennsylvania, 1965, pp. 1067-1080.
2. Berl, W. G., Hart, R. W., and McClure, F. T. "Solid Propellant Instability of Combustion, 1964 Status Report" Applied Physics Laboratory Report No. TG371-8A, Johns Hopkins University, Silver Spring, Maryland.
3. Berl, W. G., "Instability in Solid Rockets," Astronautics and Aeronautics 3, 54-62 (February 1965).
4. Angelus, T. A. "Unstable Burning Phenomena in Double-Base Propellants," ARS Progress in Astronautics and Rocketry: Solid Propellant Rocket Research, edited by M. Summerfield (Academic Press, New York, 1960), Vol. I, pp. 527-559.
5. McClure, F. T., et al, Panel Discussion: Solid-Propellant Combustion Instability, Eighth Symposium (International) on Combustion (Williams & Wilkins Co., Baltimore, 1962), pp. 904-932.
6. Horton, M. D. and McGie, M. R. "Particulate Damping of Oscillatory Combustion," AIAA J. 1, 1319-1326 (1963).
7. Horton, M. D., "Use of the One-Dimensional T-Burner to Study Oscillatory Combustion" AIAA J. 2, 1112-1118 (1964).
8. Cheng S. I. "Combustion Instability in Solid Rockets Using Propellants with Metal Additives," ARS Progress in Astronautics and Rocketry: Solid Propellant Rocket Research, edited by M. Summerfield (Academic Press, New York, 1960), Vol. I, pp. 393-422.

PRECEDING PAGE BLANK



ROCKETDYNE • A DIVISION OF NORTH AMERICAN AVIATION, INC

9. Sewell, C. J. T. "On the Extinction of Sound in a Viscous Atmosphere by Small Obstacles" *Phil. Trans. (A)* 210, 239 (1910).
10. Lamb, H., Hydrodynamics (Dover Publications, New York, 1945) 6th edition, pp. 657-661.
11. Epstein, P. S. and Carhart, R. R., "The Absorption of Sound in Suspensions and Emulsions. I Water Fog in Air" *J. Acoust. Soc. Am.* 30, 765-771 (1958).
12. Blair, D. W. "Particulate Damping of a Plane Acoustic Wave in Solid Propellant Combustion Gases," *AIAA, J. 1*, pp. 2625-2626, (1963).
13. Chow, J. C. F. "Attenuation of Acoustic Waves in Dilute Emulsions and Suspensions" *J. Acoust. Soc. Am.* 32, 2395-2401 (1964).
14. Soo, S. L. "Effect of Transport Processes on Attenuation and Dispersion in Aerosols," *J. Acoust. Soc. Am.* 32, 943-946 (1960).
15. Temkin, S. "Attenuation and Dispersion of Sound by Particulate Relaxation Processes" Brown University Report No. Nonr-562(37)/1 (Division of Engineering, Providence, R. I.) Feb. 1966.
16. Dobbins, R. A. and Temkin, S. "Measurements of Particulate Acoustic Attenuation," *AIAA J.* 2, 1106-1111, (1964).
17. Landau, L. D. and Lifshitz, E. M., Fluid Mechanics (Addison-Wesley Publishing Co., Reading, Mass. 1959), 238-240 and 298-299.
18. Cantrell, R. H. and Hart, R. W., "Interaction Between Sound and Flow in Acoustic Cavities: Mass Momentum, and Flow Considerations" *J. Acoust. Soc. Am.* 36, 697-706 (1964).
19. Rayleigh, J. W. S., The Theory of Sound (Dover Publications, New York, 1948), Vol. II, pp. 272-282.
20. Price, E. W. et al., "Low-Frequency Combustion Instability of Solid Rocket Propellants, 1 May 1963-31 May 1964," U. S. Naval Ordnance Test Station, Technical Progress Report 360, NOTS TP 3524 (China Lake, California), July 1964.



21. Watermeier L. A., Aungst, W. P., and Phaff S. P., "An Experimental Study of the Aluminum Additive Role in Unstable Combustion of Solid Rocket Propellants" Eighth Symposium (International) on Combustion (Academic Press, New York, 1963) pp. 316-325.
22. Beckstead, M. W., "Non-Acoustic Combustion Instability of Solid Propellants," Ph. D. Thesis, Department of Chemical Engineering, Salt Lake City, Utah, June 1965. Also see: Beckstead, M. W. et al, "Non-Acoustic Combustion Instability" ICRPG 2nd Combustion Conference, CPIA No. 105 (Chemical Propulsion Information Agency, Applied Physics Laboratory, Silver Spring, Md.) Vol. I, pp. 659-675.
23. Sehgal, R. and Strand, L. "A Theory of Low-Frequency Combustion Instability in Solid Rocket Motors," AIAA J. 2, 696-702 (1964).
24. Hart, R. W. and McClure, F. T. "Combustion Instability: Acoustic Interaction with a Burning Propellant Surface," J. Chem. Phys 30, 1501-1514 (1959).
25. Denison, M. R., and Baum, E., "A Simplified Model of Unstable Burning in Solid Propellants," ARS J. 31, 1112-1121 (1961).
26. Hart, R. W. and McClure, F. T. "Theory of Acoustic Instability in Solid Propellant Rocket Combustion," Tenth Symposium (International) on Combustion (Combustion Institute, Pittsburgh, Pennsylvania, 1965), pp. 1047-1065.
27. Horton, M. D., "Testing the Dynamic Stability of Solid Propellants: Techniques and Data," U.S. Naval Ordnance Test Station Report No. NOTS TP 3610, NAVWEPS Report 8596 (August 1964).
28. Eisel, J. L., et al "Preferred Frequency Oscillatory Combustion of Solid Propellants," AIAA J. 2, 1319-1322 (1964).
29. Price, E. W. "Review of the Combustion Instability Characteristics of Solid Propellants," Preprint of Paper Presented at 25th Meeting of the AGARD Combustion and Propulsion Panel, San Diego, California, April 1965.



ROCKETDYNE • A DIVISION OF NORTH AMERICAN AVIATION, INC.

30. Huebner, A. L. and Coulter, T. A. "Response of a Burning Solid Propellant to Pressure Waves of Finite Amplitude," AIAA Paper No. 66-601 June, 1966.
31. Oberg, C. L. "Acoustic Instability in Propellant Combustion" Unpublished Ph. D. Thesis, University of Utah (Department of Chemical Engineering, Salt Lake City, 1965). Also see Oberg, C. L., et al "The T-Burner: An Old Vice Overcome, a New Vice Discovered," ICPIG 2nd Combustion Conference, CPIA No. 105 (Chemical Propulsion Information Agency, Silver Spring, Md.) pp. 861-866.
32. Zink, J. W. and Delsasso, I. P., "Attenuation and Dispersion of Sound by Solid Particles Suspended in a Gas," J. Acoust Soc. Am. 30, 765-771 (1958).
33. Temkin, S. and Dobbins, R. A. "Measurement of Attenuation and Dispersion of Sound by an Aerosol" Brown University Report No. Nonr-562(37)/2 (Division of Engineering, Providence, R. I.), May 1966.
34. Dobbins, R. A. and Temkin, S. "Measurements of Particulate Acoustic Attenuation," AIAA J. 2, 1106-1111, (1964).
35. Wolfe, H. E. and Andersen, W. H. "Kinetics Mechanism and Resultant Droplet Sizes of the Aerodynamic Breakup of Liquid Drops" Aerojet-General Corporation Report No. 0395-04(18)SP, (Research and Engineering Division, Downey, California), April 1964.
36. Rabin, E., Schallenmuller, A. R., and Lawhead, R. B. "Displacement and Shattering of Propellant Droplets" Final Summary Report, Air Force Office of Scientific Research AFOSR-TR60-75 (Washington, D.C.), March 1960.
37. Dickerson, R. A. and Schuman, M. D., "Rate of Aerodynamic Atomization of Droplets" J. Spacecraft and Rockets 1, 99-100 (1965).



ROCKETDYNE • A DIVISION OF NORTH AMERICAN AVIATION INC

38. Coates, R. L., Horton, M. D. and Ryan, N. W., "T-Burner Method of Determining the Acoustic Admittance of Burning Propellants," AIAA J. 2, 1119-1122 (1964).
39. Horton, M. D. and Rice, D. W. "The Effect of Compositional Variables Upon Oscillatory Combustion of Solid Rocket Propellants" Comb. and Flame 8, 21-28 (1964).
40. Horton, M. D. and Price, E. W. "Dynamic Characteristics of Solid Propellant Combustion," Nineth Symposium (International) on Combustion (Academic Press, New York, 1963) pp. 303-309.
41. Yount, R. A. and Angelus, T. A. "Chuffing and Nonacoustic Instability Phenomena in Solid Propellant Rockets" AIAA J. 2, 1307-1313.
42. Price, E. W.: "L\* Combustion Instability," Proceedings of the First ICRPG Combustion Instability Conference, Vol. I, CPIA No. 68, January 1965.



ROCKETDYNE • A DIVISION OF NORTH AMERICAN AVIATION INC

PUBLICATIONS RESULTING FROM WORK PERFORMED

1. Huebner, A. L., and T. A. Coulter, "Response of a Burning Solid Propellant to Pressure Waves of Finite Amplitude," presented at the AIAA Second Propulsion Joint Specialist Conference, Colorado Springs, Colorado, 13 to 17 June 1966, AIAA Preprint 66-601.
2. Oberg, C. L., "Effects of Aluminum on Solid Propellant Combustion Instability," to be presented at Third ICRPG Combustion Conference, John F. Kennedy Space Center, Florida, 17 to 20 October 1966.



ROCKETDYNE • A DIVISION OF NORTH AMERICAN AVIATION, INC

## APPENDIX A

### NOMENCLATURE

A	= defined by Eq. B-11
$a_0$	= isentropic sound velocity, $\gamma p_0 / \rho_0$
$c_m$	= ratio of total particulate mass per unit volume to gas density
$c_p$	= heat capacity at constant pressure for the gas
$c'_p$	= heat capacity of particulate matter
$c_s$	= heat capacity (average) of solid propellant
$c$	= isentropic sound velocity, $\gamma p_0 / \rho_0$
$c_d$	= isentropic sound velocity in droplet
$c^*_0$	= characteristic exit velocity of the gas (isentropic)
D	= motor port diameter
$D_{ij}$	= mean particle size, defined by Eq. 10
$D_s$	= diameter of droplet located on burning surface
$D_v$	= diameter of droplet located in main gas volume
$E_f$	= activation energy for overall gas-phase reaction
$E_w$	= activation energy for surface vaporization
$\tilde{E}$	= defined by Eq. B-11
$\dot{E}$	= rate of energy dissipation
$\dot{E}_{part}$	= $\dot{E}$ due to particulate damping
$\dot{E}_{therm}$	= thermal contribution to $\dot{E}$



ROCKETDYNE • A DIVISION OF NORTH AMERICAN AVIATION, INC

$\dot{E}_{vis}$	= viscous contribution to $\dot{E}$
$f$	= oscillatory frequency
$Im \{ \}$	= imaginary part of enclosed quantity
$j$	= $(-1)^{1/2}$
$K_n$	= ratio of burning surface area throat area
$k$	= thermal conductivity
$k_d$	= $k$ of droplet
$L$	= motor length
$L^*$	= ratio of chamber volume to throat area
$l$	= motor length
$m_0$	= time-average mass flux
$\tilde{m}$	= perturbed mass flux
$N_s$	= number of drops in burning surface
$N_v$	= number of drops in chamber volume
$n$	= burning rate exponent
$n$	= integer
$n$	= distribution in particle size
$Pr$	= $\mu C_p/k$
$p_0$	= time average pressure
$\tilde{p}$	= perturbed pressure
$\hat{p}$	= amplitude of $\tilde{p}$
$q$	= defined by Eq. B-11



ROCKETDYNE • A DIVISION OF NORTH AMERICAN AVIATION, INC.

- R = ideal gas constant  
Re { } = real part of enclosed quantity  
r = burning rate of propellant  
r = radius of particle  
 $\bar{r}$  = mean particle radius  
S = defined by Eq. B-11  
 $S_b$  = burning surface area  
 $T_o$  = time average temperature  
 $\tilde{T}$  = perturbed temperature  
 $T_{fo}$  =  $T_o$  of combustion products  
 $T_i$  = initial temperature of unburned propellant  
 $T_{wo}$  =  $T_o$  at burning surface  
 $\tilde{T}_f$  =  $\tilde{T}$  of combustion products  
t = time  
 $u_o$  = time-average gas velocity  
V = chamber volume (gas phase)  
 $\alpha$  = growth constant  
 $\alpha'$  = thermal diffusivity  
 $\alpha_b$  = growth constant obtained during burning  
 $\alpha_l$  = thermal expansion coefficient of droplet  
 $\alpha_{nb}$  = growth constant obtained after burn-out  
 $\bar{\alpha}$  = reduced attenuation coefficient, Eq. 1



ROCKETDYNES • A DIVISION OF NORTH AMERICAN AVIATION INC

$\beta$	= $\omega - j \alpha$
$\beta_l$	= compressibility of droplet
$\gamma$	= ratio of heat capacities for gas phase, $C_p/C_v$
$\gamma_l$	= ratio of heat capacities for droplet
$\gamma'$	= propagation constant, Eq. B-5
$\delta$	= ratio of gas density to particle density
$\epsilon$	= $\tilde{p}/p_0$
$\theta$	= phase angle
$\lambda$	= defined by Eq. B-11
$\kappa$	= $\tilde{m}/m_0$
$\mu$	= gas viscosity
$\mu_l$	= droplet viscosity
$\nu$	= $\mu/p_0$
$\pi$	= 3.14159
$\rho$	= density
$\rho_0$	= time-average $\rho$
$\rho_g$	= time-average gas density
$\rho_l$	= time-average droplet density
$\rho_s$	= density (average) of solid propellant
$\sigma$	= surface tension
$\tau$	= defined by Eq. B-11
$\tau_D$	= $(D_v^2 \rho_l)/(8\mu)$



**ROCKETDYNE** • A DIVISION OF NORTH AMERICAN AVIATION, INC.

- $\tau_t$  =  $(5 \text{ Pr } C_p' \tau_b) / (2 C_p)$   
 $Y_n$  = virtual acoustic admittance of nozzle  
 $\Phi_v$  = viscous dissipation function  
 $\omega$  = angular frequency,  $2\pi f$



ROCKETDYNE • A DIVISION OF NORTH AMERICAN AVIATION, INC

## APPENDIX B

### ANALYSIS OF NONACOUSTIC INSTABILITY

Quasi-periodic agglomeration and shedding of aluminum from the burning surface at low frequencies has often been reported (Ref. 20 and 21). Also it has often been suggested that this process may act to drive nonacoustic instability. In the nonacoustic frequency range particulate damping is expected to be unimportant due to its strong dependence on frequency. Therefore, the aluminum may have a destabilizing influence in this frequency region. The effect of the aluminum is difficult to estimate analytically. Some progress was made in determining the source of the quasi-periodicity, however. In doing so, a detailed analysis of non-acoustic instability was developed. Significantly, it was found that nonacoustic instability is intimately related to acoustic instability rather than completely divorced as other investigators have concluded. The dynamic behavior of a motor exhibiting nonacoustic instability was analyzed. Previous analyses of nonacoustic instability have made use of the ballistic equation, in perturbation form, and a model for the combustion behavior (Ref. 20 and 21). Following this approach, but without specifying the combustion model, a characteristic equation was obtained for the frequency.

It is assumed that: (1) the mode is a bulk mode; (2) the gas behavior is isentropic; the isothermal case is obtained by setting  $\gamma$  to unity; (3) the isentropic expression for flow through the nozzle is valid in the perturbed case. This is equivalent to the zero length-nozzle approximation for the acoustic admittance of a nozzle. The approximation is good because the equivalent wavelength is infinite; and (4) the rate of volume



ROCKETDYNE • A DIVISION OF NORTH AMERICAN AVIATION, INC.

increase, due to time-average burning is negligible. With these assumptions the perturbed equation becomes:

$$\frac{L^* c_0^*}{c^2} \frac{d}{dt} \left( \frac{\tilde{p}}{p_0} \right) = \frac{\tilde{m}}{m_0} - \left( \frac{\gamma+1}{2\gamma} \right) \frac{\tilde{p}}{p_0} \quad (B-1)$$

Assuming an exponential time dependence, i.e.,  $e^{j\beta t}$ . Equation B-1 is rearranged to give

$$\frac{\tilde{m}}{m_0} = \left( j\beta \frac{L^* c_0^*}{c^2} + \frac{\gamma+1}{2\gamma} \right) \frac{\tilde{p}}{p_0} \quad (B-2)$$

If use is made of the definition of the response function, in perturbation form, we obtain:

$$\mu/\epsilon = j\beta \frac{L^* c_0^*}{c^2} + \frac{\gamma+1}{2\gamma} \quad (B-3)$$

Therefore, the response function explicitly defines the time dependence,  $\beta$ . The frequency of oscillation is determined by the imaginary part,  $\text{Im} \{\mu/\epsilon\}$ , and whether the oscillations grow or decay is determined by the real part,  $\text{Re} \{\mu/\epsilon\}$ .

Equation B-3 can also be obtained by an acoustic approach. For low-velocity mean flow in the main cavity, the mean flow may be neglected as long as it is taken into account at the boundaries by using virtual



ROCKETDYNE • A DIVISION OF NORTH AMERICAN AVIATION, INC.

acoustic-admittance values at these positions. Assuming the wave behavior to be described by the conventional wave equation, solutions were obtained for two motor geometries.

The first geometry considered was cylindrical with propellant being burned on the curved boundary, a rigid boundary at the head end, and a sonic nozzle at the aft end. Without difficulty it is found that

$$-\frac{\gamma'}{\rho_0 \beta} \tanh j\gamma' l = Y_n \quad (B-4)$$

where  $\gamma'$  is given by

$$j \frac{p_0}{\rho_0 u_0 \beta} \left( \frac{\beta^2}{c^2} - \gamma'^2 \right)^{1/2} \frac{J_1 \left\{ \left( \frac{\beta^2}{c^2} - \gamma'^2 \right)^{1/2} \frac{D}{2} \right\}}{J_0 \left\{ \left( \frac{\beta^2}{c^2} - \gamma'^2 \right)^{1/2} \frac{D}{2} \right\}} = \frac{\mu}{\epsilon} \quad (B-5)$$

The argument of the Bessel functions is normally sufficiently small that Eq. B-5 becomes:

$$j \frac{p_0}{\rho_s r} \frac{D}{4\beta} \left( \frac{\beta^2}{c^2} - \gamma'^2 \right) = \frac{\mu}{\epsilon} \quad (B-6)$$

This equation may be solved for  $\gamma'$ , i.e.,

$$\gamma' = \frac{\beta}{c} + j \frac{c}{2L^* c_0^*} \frac{\mu}{\epsilon} \quad (B-7)$$



ROCKWELL INTERNATIONAL • A DIVISION OF NORTH AMERICAN AVIATION, INC.

Equation B-4 in conjunction with Eq. B-7, determines the complex frequency,  $\rho$ .

In the case of interest, the virtual nozzle admittance is sufficiently small that

$$\tanh j \gamma' l \approx j (\gamma' l - n\pi) \quad n = 0, 1, 2, \dots$$

$$= - \frac{\rho_0 \beta}{\gamma'} Y_n \quad (B-8)$$

The values of  $n$  correspond to various longitudinal modes. With the zero-length nozzle equation, and setting  $n = 0$  for the zeroth mode, it is found from Eq. B-8 that

$$\frac{\mu}{\epsilon} = j \beta \frac{L^* c_0^*}{c^2} + \frac{\gamma+1}{2\gamma} \quad (B-9)$$

which is identical with Eq. B-3. Thus the zeroth mode corresponds to the bulk mode previously treated with the ballistic equation. Note that for a closed cavity with no gains or losses,  $\beta = 0$  for the zeroth mode. Therefore, there is no analogous mode in the simple case. Also, it is observed that several approximations were made in order to obtain the results given in Eq. B-9. All of the approximations are usually valid; however, if any of the approximations are invalid then the more general equations must be used. Indeed, in the latter case, use of the perturbed ballistic equation is incorrect.



ROCKETDYNE • A DIVISION OF NORTH AMERICAN AVIATION, INC

The second configuration considered was also a cylindrical geometry but the curved walls were rigid, propellant was burned at the head end and a sonic nozzle was located at the aft end. Again using the zero-length nozzle approximation, solution of the acoustic problem leads to the characteristic equation

$$\tan \frac{\theta l}{c} = j \frac{\frac{\gamma+1}{2\gamma} - \frac{u}{\epsilon}}{\frac{c_0 * K_n}{c} + \frac{c}{c_0 * K_n} \left( \frac{\gamma+1}{2\gamma} \right)} \approx \frac{\theta l}{c} - n \pi \quad (B-10)$$

With reasonable values of  $K_n$ , the zeroth mode is again given by an equation identical with Eq. B-3.

The foregoing results emphasize the relationship between acoustic and nonacoustic instability. Indeed, they suggest that combustion models for acoustic instability (e.g., Ref. 24 and 25) may apply to nonacoustic instability as well. The value of this suggestion was tested with the Denison-Baum model for acoustic instability, (Ref. 25).

For an exponential time dependence (i.e.,  $e^{j\beta t}$ ), the Denison-Baum model may be solved to obtain the following response function:

$$\mu/\epsilon = \frac{-n \lambda A}{q + s - \frac{jA}{\beta T} (1 + s)} \quad (B-11)$$

where

$$s = 1/2 \left[ 1 + (1 + 4j\beta T)^{1/2} \right] \quad q = 1 + A (1 - \lambda)$$



ROCKETDYNE • A DIVISION OF NORTH AMERICAN AVIATION, INC

$$\lambda = \frac{C_p T_{f_0}}{\xi C_s (T_{w0} - T_i)}$$

$$\xi = n + 1 + E_f / 2RT_{f_0}$$

$$A = \frac{E_w}{RT_{w0}} \left( 1 - \frac{T_i}{T_{w0}} \right)$$

$$\tau = \frac{\alpha}{r_0^2}$$

$T_f$  = flame temperature

$T_i$  = bulk temperature of propellant

The parameters  $\lambda$ ,  $n$ , and  $S$  are equivalent to  $\alpha$ ,  $n/2$ , and  $\lambda$ , respectively, in Denison-Baum nomenclature.

Hart and McClure (Ref. 26) indicate that the Denison-Baum results are quite similar to their own. However, no direct comparison of either model has been made with experimental data. Therefore, extensive calculations were made with Eq. B-11 to test its ability to describe response-function data.

Perhaps the best data available from which to calculate the  $Re \left\{ \frac{u}{\epsilon} \right\}$  are reported by Horton in Ref. 27 from T-burner firings. Using Horton's data, the  $Re \left\{ \frac{u}{\epsilon} \right\}$  was calculated from the equation

$$Re \left\{ \frac{u}{\epsilon} \right\} = \frac{p_0}{2r \rho_s c} \left( \frac{\alpha_b - \alpha_{n_b}}{f} \right) \quad (B-12)$$

Similar equations are widely used; an equivalent equation is developed by Cantrell (Ref. 18). The data for  $\alpha_{n_b}$  were plotted as a function of frequency and a smooth curve drawn through the data. An example of this



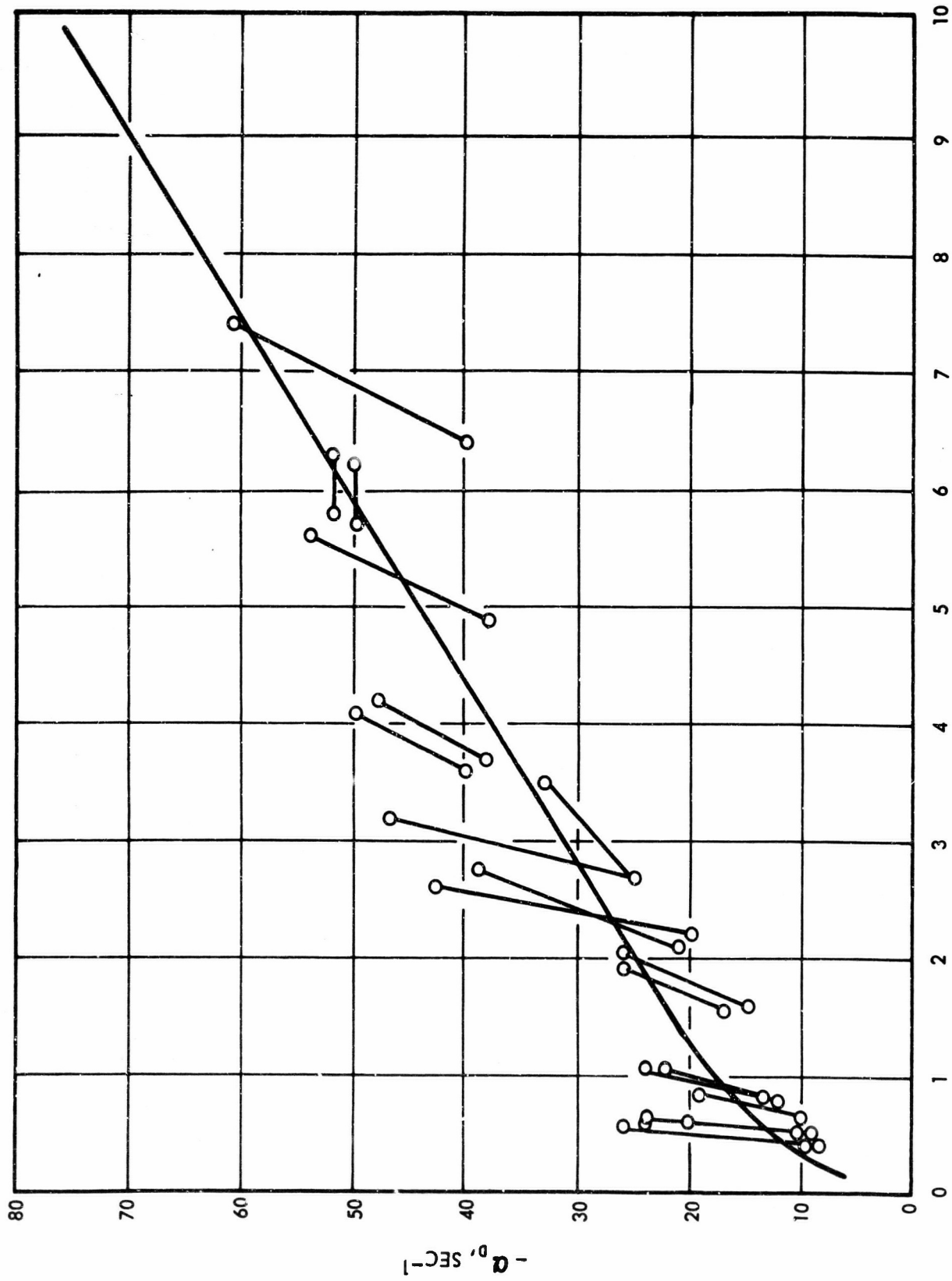
ROCKETDYNE • A DIVISION OF NORTH AMERICAN AVIATION, INC

procedure is shown in Fig. B-1. In this figure, lines are drawn connecting pairs of data points; each connected pair of points represents the initial and final values of  $\alpha_{nb}$  reported by Horton. The smooth curve through the data has been drawn to approach zero as the frequency approaches zero. This was done because, whatever the damping mechanism, the damping coefficient is expected to vanish at zero frequency. The smooth curve was then used to define a value of  $\alpha_{nb}$  to be used in Eq. B-12 with the  $\alpha_b$  data, thereby correcting for frequency shifts between the  $\alpha_b$  and  $\alpha_{nb}$  measurements as well as smoothing the  $\alpha_{nb}$  data.

Thus, experimental values of  $\text{Re} \left\{ \frac{\mu}{\epsilon} \right\}$  were calculated for four different propellants and are presented in Fig. B-2 through B-5. The data were obtained at a mean pressure of 200 psi. The propellants were designated as A-13, A-14, A-15 and A-16 by NOTS. Each was of the PBAA/AP type. A-15 and A-16 contained copper chromite catalyst while A-13 and A-14 contained none. Propellants A-13 and A-15 contained 76-percent, 80-micron AP, while A-14 and A-16 contained the same amount of 15-micron AP. On these plots are shown curves through the experimental points which were calculated from the theoretical expression. The curves, which describe the experimental values rather well, were obtained by varying the parameters A and q in Eq. B-11 until the best fit was obtained. Although a rather good description of the experimental values is obtained, the model is somewhat unsatisfactory since the curves correspond to unusually high activation energies for the surface decomposition (65 to 100 kcal/mole-K). However, this activation energy must be considered to be an effective value since the model approximates the heterogeneous propellant by a homogeneous solid. Therefore, perhaps the activation energy required to fit the experimental  $\text{Re} \left\{ \frac{\mu}{\epsilon} \right\}$  values is not unreasonable. Also, there is no doubt that the model can qualitatively describe the experimental values. It was concluded that the model was very successful for these purposes.



ROCKETDYNE • A DIVISION OF NORTH AMERICAN AVIATION, INC.



B-8

R-6654

Figure B-1. NOTS T-Burner Decay-Rate Data



ROCKETDYNE • A DIVISION OF NORTH AMERICAN AVIATION, INC

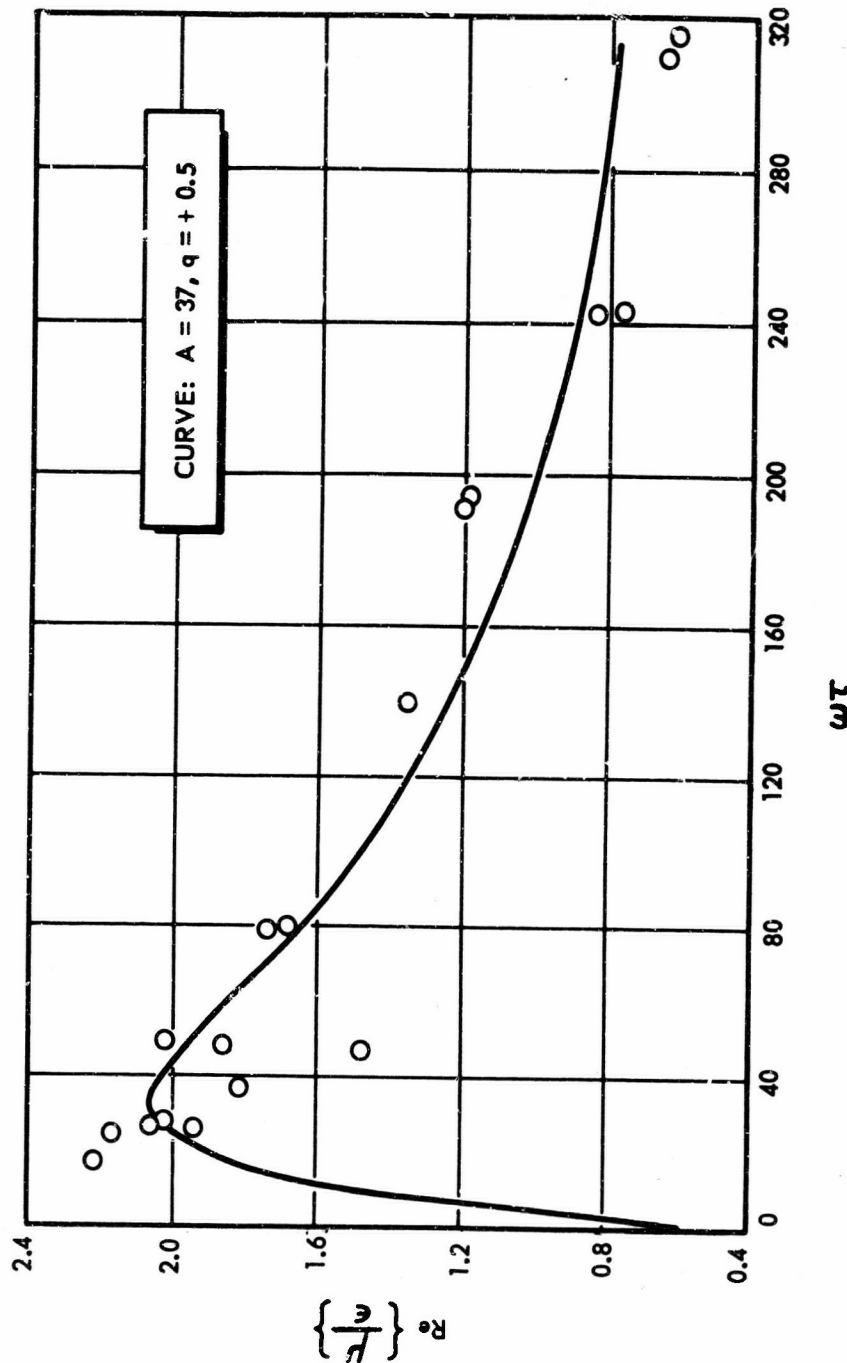


Figure B-2. Experimental Response Function From NTS Data on A-13 Propellant With Theoretical Curve Through Data



ROCKETDYNE • A DIVISION OF NORTH AMERICAN AVIATION, INC.

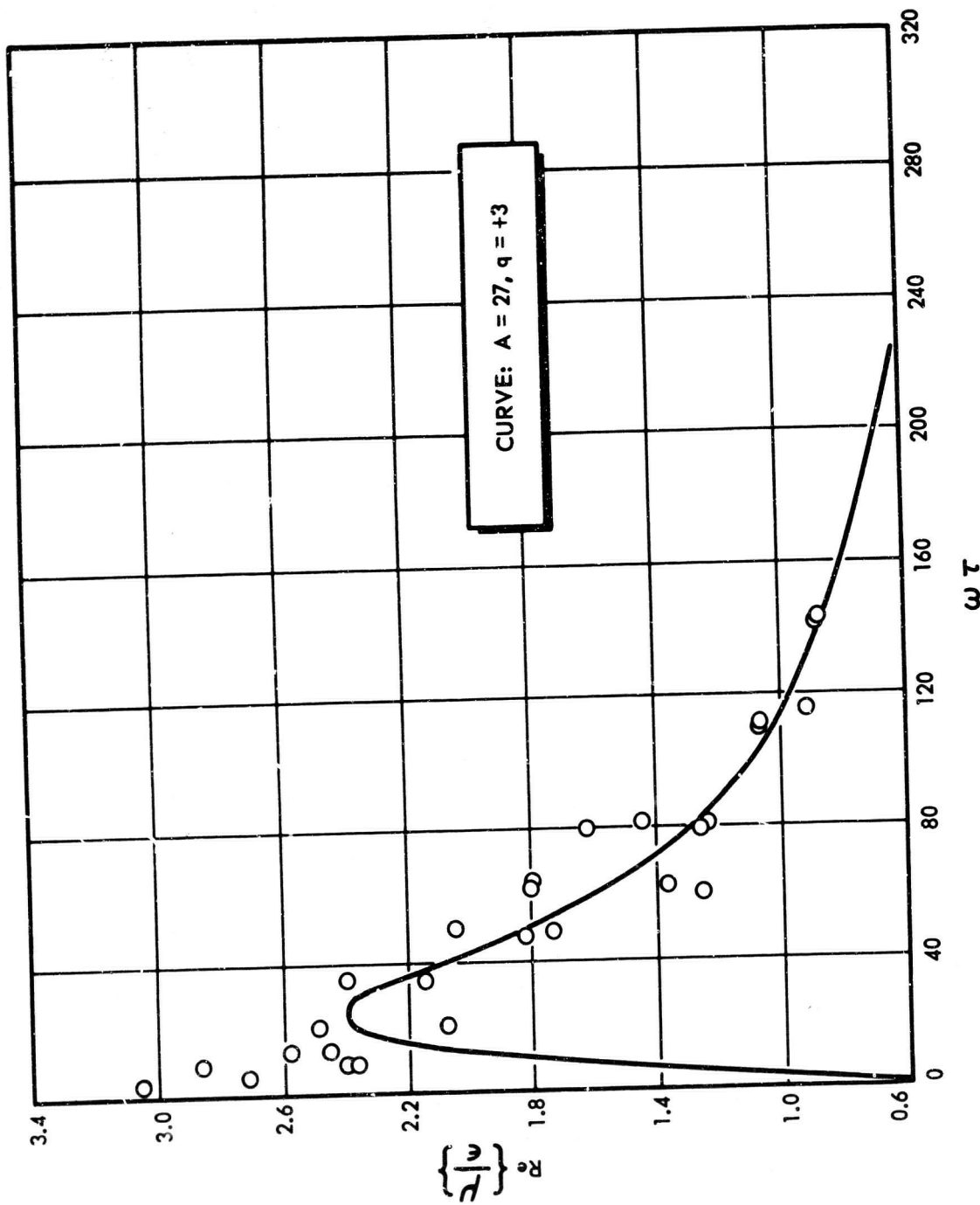


Figure B-3. Experimental Response Function From NOTS Data on A-14 Propellant With Theoretical Curve Through Data



ROCKETDYNE • A DIVISION OF NORTH AMERICAN AVIATION, INC.

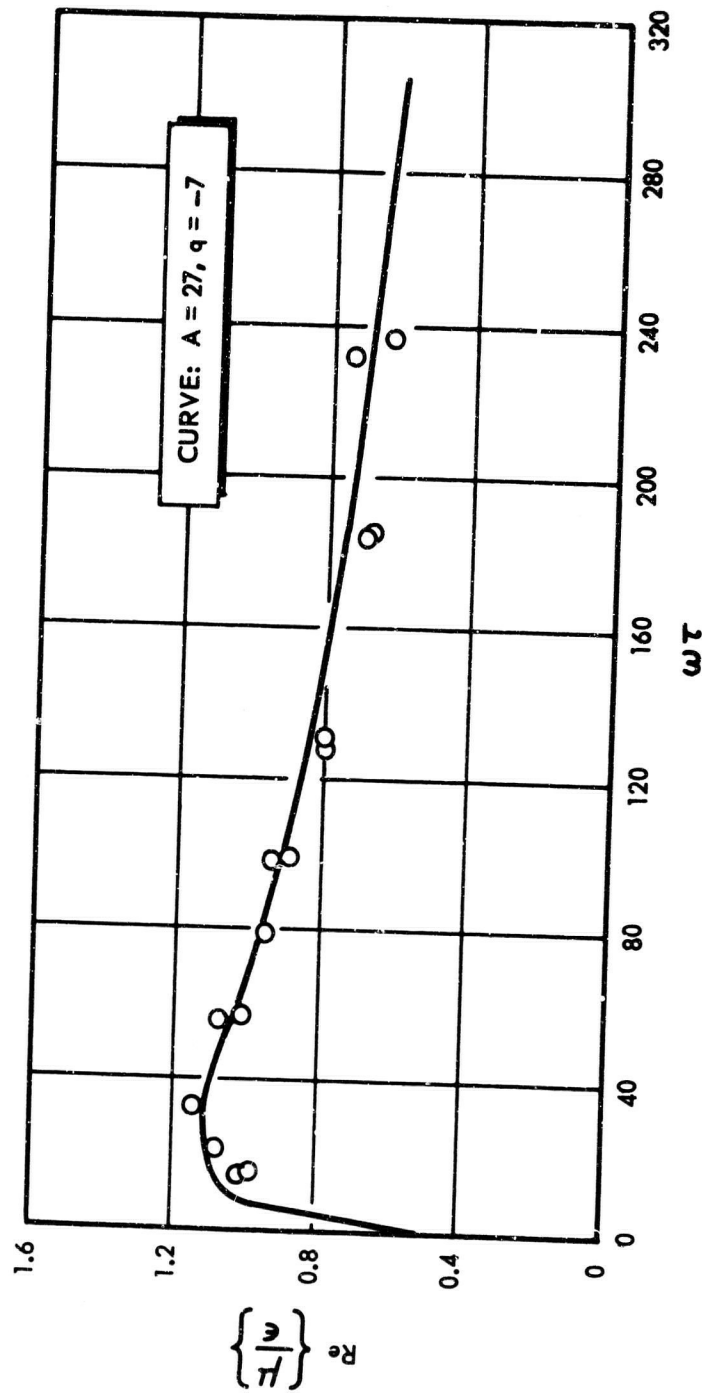


Figure B-4. Experimental Response Function From NOTS Data on A-15 Propellant With Theoretical Curve Through Data



ROCKETDYNE • A DIVISION OF NORTH AMERICAN AVIATION INC.

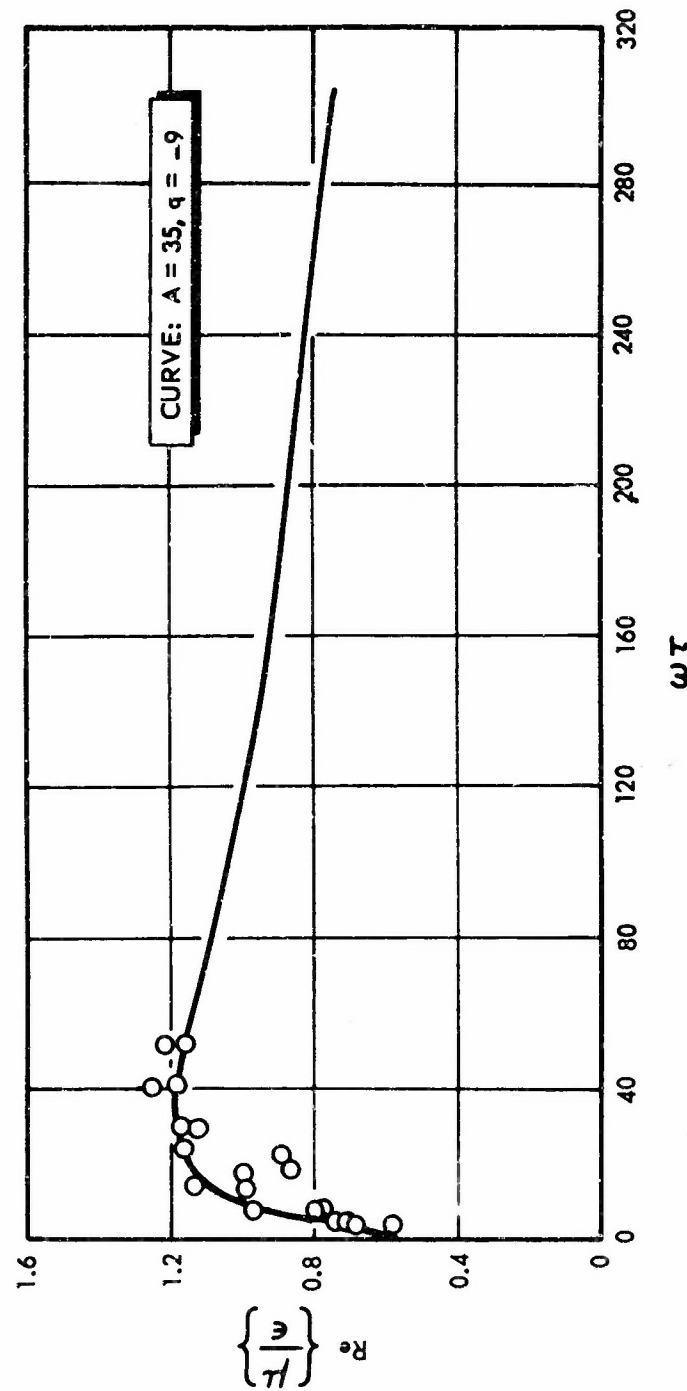


Figure B-5. Experimental Response Function From NOTS Data on A-16 propellant With Theoretical Curve Through Data



ROCKETDYNE • A DIVISION OF NORTH AMERICAN AVIATION INC

It should be mentioned that the high-frequency limitation of the Denison-Baum model is no problem for the propellants considered. According to the criterion specified by Hart (Ref. 26), the model was estimated to become invalid above  $\omega\tau \approx 240$  for each propellant. Nearly all of the data fall below this value of  $\omega\tau$ .

A second detailed comparison was made with nonacoustic instability data of Beckstead (Ref. 22). He has studied the behavior of several propellants in a low L\* motor. In the motor, propellant was burned in one end of a cylindrical cavity and a sonic nozzle was contained in the other end. He reports values of L\*, frequency, and mean pressure during instability, and, therefore, provides sufficient information to calculate  $\text{Im}\left\{\frac{\mu}{\epsilon}\right\}$  from Eq. B-3. Other investigators have not reported these data in sufficient detail to calculate  $\text{Im}\left\{\frac{\mu}{\epsilon}\right\}$ . In Fig. B-6 are presented the  $\text{Im}\left\{\frac{\mu}{\epsilon}\right\}$  obtained from Beckstead's results for three of his propellants and plotted in the format used by him. In this format a mean-pressure effect in the data is apparently suppressed. Beckstead's propellants were of the PBAA/AP type with two percent copper chromite catalyst. Propellants F, TF, and XF contained 0, 5, and 10 percent aluminum and 80, 75, and 70 percent AP, respectively. On Fig. B-6 is shown a curve through the experimental values calculated from Eq. B-3. Again the values of A and q in Eq. B-11 were varied until a best fit was obtained. As with the T-burner results, the model describes the experimental points rather well. However, contrary to the comparison with T-burner results, an activation energy for the surface decomposition as low as 27 kcal/mole-°K could be used to calculate the best-fit curve. Again it was concluded that the model describes the experimental results rather well.

Since the Denison-Baum model seemed fully adequate to at least qualitatively describe unstable combustion, several qualitative features observed in non-acoustic instability studies were considered. In each case an adequate explanation was obtained. An example is the preferred frequency reported by NOTS.



ROCKETDYNE • A DIVISION OF NORTH AMERICAN AVIATION INC

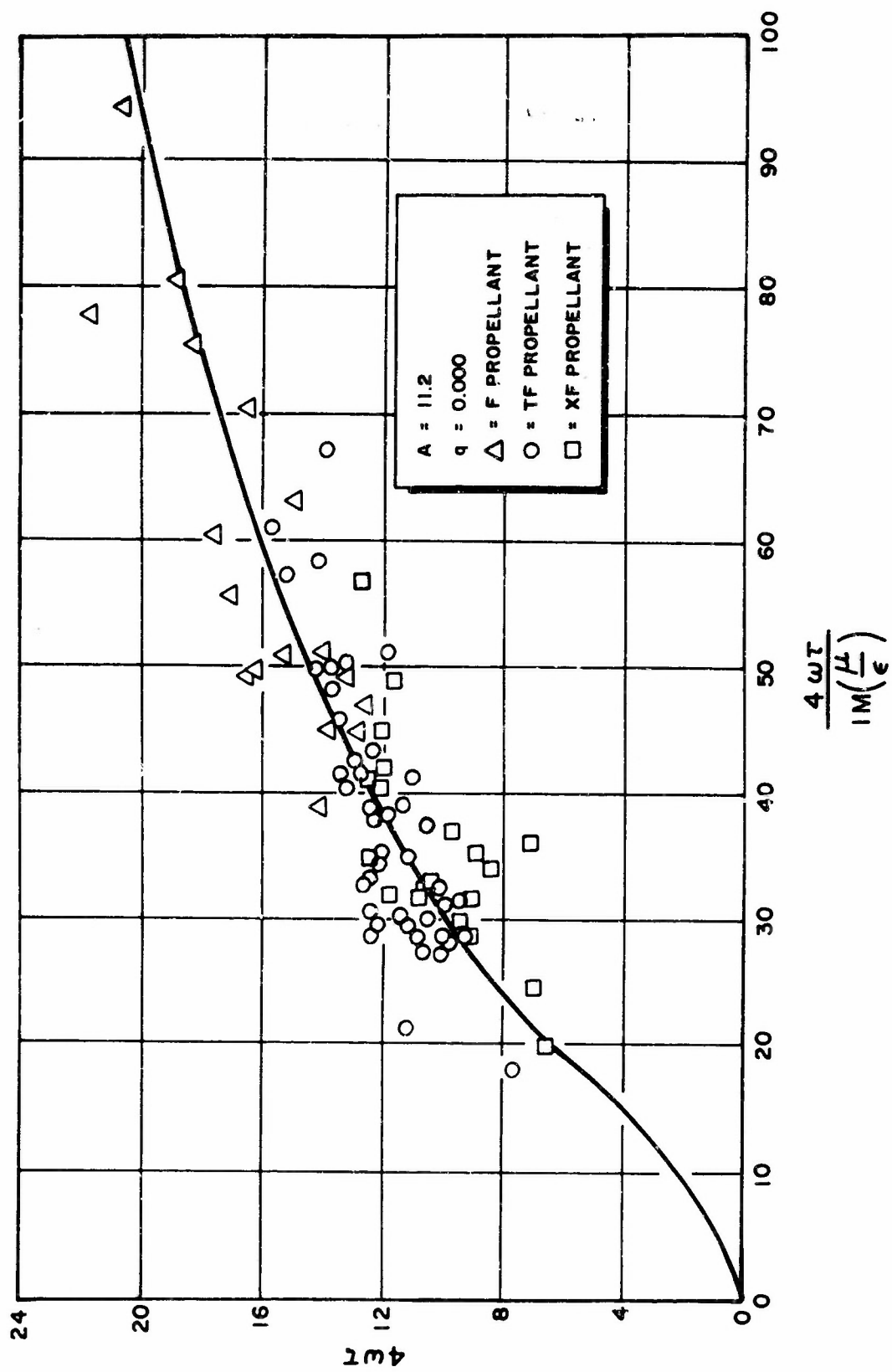


Figure B-6. Comparison of Theory With Experimental L Data From Ref. 22



ROCKETDYNE • A DIVISION OF NORTH AMERICAN AVIATION, INC

NOTS uses two kinds of experimental motors in their preferred frequency work. One is the L\* motor, which is similar to Beckstead's motor, and the other a very long T-burner, denoted as the LE burner (Ref. 20, 28, and 42). In the L\* burner, it is found that frequency correlates well with mean pressure in the motor, only a limited band of frequencies being observed. Beckstead has pointed out that there is an L\* dependence in this band of frequencies (Ref. 22). Yount (Ref. 41) has reported no L\* dependence; however, this may be attributed to the range of L\* values in which he worked. Yount's data also correlate on a frequency-mean pressure plot. Beckstead found a similar relationship.

The L\*-(nonacoustic) instability data may be explained as follows. When the L\* and/or pressure are reduced, the frequency, or  $\omega\tau$ , is increased in accord with  $\text{Im}\{\mu/\epsilon\}$  for the particular propellant. Simultaneously, the  $\text{Re}\{\mu/\epsilon\}$  is increased as  $\omega\tau$  increases. When  $\text{Re}\{\mu/\epsilon\}$  exceeds the losses in the system, i.e.,  $y+1/2y$  (or unity for an isothermal system if the only loss is the nozzle), the motor becomes unstable. Continued increase of  $\omega\tau$  results in large values of  $\text{Re}\{\mu/\epsilon\}$ , and the motor becomes so unstable that chuffing results. This description is consistent with experimental observations.

In the second kind of experiment carried out by NOTS, propellant is burned in a T-burner ranging in length up to 60 feet. In this system, the mean pressure is allowed to increase slowly during the run. The frequency is determined by the acoustics of the cavity. It is found that instability develops when the pressure becomes sufficient and then ceases at a higher pressure (Ref. 20, 28, and 42).

In this motor, the losses are determined by the acoustics of the cavity, these being frequency dependent. Viewed in terms of the  $\text{Re}\{\mu/\epsilon\}$ , the



experiment begins at a large value of  $\omega\tau$ , because of the low pressure and fixed frequency. As the pressure rises,  $\omega\tau$  diminishes and  $Re\{\mu/\epsilon\}$  increases toward the maximum. There will be a value of  $Re\{\mu/\epsilon\}$  which corresponds to the losses in the system; when this value is exceeded, the motor will oscillate. As  $\omega\tau$  continues to decrease, the oscillatory amplitude will increase and then diminish. When  $Re\{\mu/\epsilon\}$  again drops below that necessary to overcome the losses, the oscillation will cease. If the motor length is changed, the frequency is changed, and also the losses. The motor will again oscillate in the range of  $\omega\tau$  values for which  $Re\{\mu/\epsilon\}$  exceeds that corresponding to the losses. If the losses are sufficiently large, there will be no value of  $Re\{\mu/\epsilon\}$  at which the losses are exceeded.

The preferred frequencies will coincide, for the two kinds of experiments only if the losses are equivalent in the two systems. The preferred frequency plot, i.e., the frequency-mean pressure plot, shows the variation of the  $\omega\tau$  at the stability limit with mean pressure. If  $\{\mu/\epsilon\}$  and the losses vary only weakly with mean pressure, the preferred frequency will approximately correspond to a constant  $\omega\tau$  at the stability limit.

NOTS has also reported observing a phase difference between the oscillatory light emission from the propellant surface and the oscillatory pressure (Ref. 20, 28, 29, and 42). This phase shift has been explained in terms of the preferred frequency concept. The observation is also explainable in terms of the current analytical model.

In the long T-burner NOTS observed: an oscillating light signal which lags the pressure as the oscillations begin; as the pressure oscillations reached a maximum, the phase angle became zero; and, finally, a phase



ROCKETDYNE • A DIVISION OF NORTH AMERICAN AVIATION INC

lead was observed while the oscillation diminished (Ref. 28, 29, and 42). In the L\* burner, only a phase lead is observed. An explanation may be obtained if it is assumed that the light oscillations correspond to oscillations in flame temperature. The Denison-Baum model gives:

$$\frac{\tilde{T}_f}{T_{fe}} = \frac{(\mu - n)}{\epsilon} \frac{\tilde{p}}{p_0} \quad (B-13)$$

From Eq. B-13, the phase angle between the perturbed temperature and pressure is given by:

$$\tan \theta = \frac{\text{Im} \{ \mu/\epsilon \}}{\text{Re} \{ \mu/\epsilon \} - n} \quad (B-14)$$

As noted previously, in the long T-burner,  $\omega\tau$  is large initially and diminishes. In relation to Eq. B-14, the numerator of the right side is negative and the denominator positive at large  $\omega\tau$ . As  $\omega\tau$  diminishes,  $\text{Im} \{ \mu/\epsilon \}$  diminishes, becoming zero at the  $\omega\tau$  corresponding to the maximum in  $\text{Re} \{ \mu/\epsilon \}$  while the denominator remains positive. Both the numerator and denominator are positive for values of  $\omega\tau$  less than that of the maximum in  $\text{Re} \{ \mu/\epsilon \}$ . Thus, Eq. B-14 predicts phase angle behavior identical with that observed, i.e., the phase angle is initially negative, then diminishes and becomes positive.

With regard to the low L\* data, the motor is unstable only in the vicinity of the stability limit, i.e., in the region where  $\text{Re} \{ \mu/\epsilon \} = \gamma + 1/2\gamma$ , assuming nozzle losses dominate. In this region, the phase angle is positive, corresponding to the observed values.



ROCKETDYNE • A DIVISION OF NORTH AMERICAN AVIATION, INC

At NOTS and elsewhere, quasi-periodic shedding of aluminum from the burning surface of aluminized propellants has been observed. The nominal frequency of this shedding is in the range of nonacoustic instability. Such shedding is observed when there is no acoustic cavity in the vicinity of the propellant; i.e., the propellant is burned in the open or in a bomb. However, the dense cloud of burning aluminum leaving the burning surface will be able to reflect local disturbances generated by the combustion back to the surface where the disturbance can be amplified. The frequency components of the disturbance near the maximum in  $Re\{\mu/\epsilon\}$  (actually the growth constant for the surface) will be amplified to the greatest degree. It seems likely, therefore, that the frequency of the shedding will tend toward that corresponding to the maximum in the response function.

From this study of nonacoustic instability, it was concluded that a rather good analytical description of the phenomena had been developed. Also, the utility of the Denison-Baum combustion model is very evident.



**ROCKETDYNE** • A DIVISION OF NORTH AMERICAN AVIATION INC

**APPENDIX C**

**EXPERIMENTAL DATA**



ROCKETDYNE • A DIVISION OF NORTH AMERICAN AVIATION, INC

TABLE C-1

GROWTH CONSTANT-FREQUENCY DATA OBTAINED BY FIRING IGNITER  
ONLY AND PULSING WITH A NO. 2374 SQUIB

Test No.	$P_0$ , psig	$-\alpha_{nb}$ seconds $^{-1}$	$f_{nb}$ , cps	L, inches
127	200	36.0	1190	9
128	200	46.0	1230	9
129	200	56.0	1260	9
96	200	19.0	610	15
98	200	17.0	620	15
92	200	13.0	360	21
93	200	15.0	390	21
94	200	13.0	390	21
108	200	4.0	170	41
109	200	3.3	180	41
110	200	4.0	180	41
130	400	39.0	1290	9
131	400	42.0	1230	9
132	400	47.0	1240	9
77	400	16.0	660	15
79	400	13.0	620	15
80	400	11.0	560	15
44	400	16.0	430	21
83	400	7.9	340	21
84	400	8.2	340	21
85	400	9.8	350	21
111	400	5.6	170	41
114	400	6.5	170	41
115	400	6.2	170	41
133	600	24.0	1140	9
134	600	28.0	1120	9



ROCKETDYNE • A DIVISION OF NORTH AMERICAN AVIATION, INC

TABLE C-1  
(Concluded)

Test No.	$p_0$ , psig	$-\alpha_{nb} \text{ seconds}^{-1}$	$f_{nb}$ , cps	L, inches
99	600	11.0	550	15
100	600	16.0	510	15
101	600	16.0	500	15
86	600	9.4	350	21
87	600	11.0	350	21
88	600	10.0	350	21
116	600	5.5	170	41
117	600	5.5	170	41
118	600	6.5	170	41



ROCKETDYNE • A DIVISION OF NORTH AMERICAN AVIATION, INC

TABLE C-2

## GROWTH CONSTANT-FREQUENCY DATA FROM A-PROPELLANT

Test No.	$p_0$ , psig	$\alpha_b$ , seconds $^{-1}$	$f_b$ , cps	$-\alpha_{nb}$ , seconds $^{-1}$	$f_{nb}$ , cps	L, inches
119	200	16.0	2260	24.0	1970	9
121	200	11.0	2160	20.0	1930	9
122	200	19.0	2220	23.0	1950	9
138	200	11.0	2220	26.0	1920	9
140	200	15.0	2200	22.0	1950	9
144	200	9.0	1200	15.0	1040	15
177	200	14.0	1230	19.0	1060	15
178	200	20.0	1250	22.0	910	15
8	200	8.5	805	12.0	590	21
9	200	7.4	800	12.0	540	21
10	200	8.1	780	12.0	530	21
16	200	7.7	700	12.0	670	21
25	200	7.2	710	15.0	660	21
26	200	5.2	760	14.0	640	21
29	200	9.1	790	12.0	600	21
33	200	8.0	790	12.0	600	21
34	200	7.7	790	11.0	610	21
120	200	2.1	380	8.4	340	41
122	200	5.0	380	8.5	290	41
124	200	4.3	370	7.7	300	41
125	400	-61.0	1950	60.0	1500	9
136	400	-47.0	1990	75.0	1620	9
142	400	7.6	2260	12.0	2060	9
45	400	-14.0	790	24.0	560	21
46	400	-7.1	840	21.0	680	21
126	400	-4.4	380	8.9	250	41
137	400	-6.0	370	5.9	220	41
139	400	-6.9	380	6.6	220	41
141	400	-7.3	380	7.6	210	41



ROCKETDYNE • A DIVISION OF NORTH AMERICAN AVIATION, INC.

TABLE C-2  
(Concluded)

Test No.	$p_0$ , psig	$\alpha_b'$ , seconds <sup>-1</sup>	$f_b'$ , cps	$-\alpha_{nb}'$ , seconds <sup>-1</sup>	$f_{nb}'$ , cps	L, inches
170	600	-52.0	2150	65.0	1800	9
174	600	-50.0	2070	53.0	1830	9
176	600	-39.0	2320	53.0	1750	9
66	600	-28.0	1150	30.0	1070	15
68	600	-36.0	1130	41.0	1020	15
69	600	-38.0	1170	42.0	1040	15
71	600	-32.0	1160	41.0	1060	15
65	600	-19.0	800	29.0	730	21
67	600	-14.0	780	22.0	600	21
70	600	-28.0	800	30.0	720	21
143	600	-9.2	210	—	—	41
171	600	-7.0	400	3.5	220	41
173	600	-7.5	400	4.7	210	41
175	600	-7.2	400	5.6	230	41



ROCKETDYNE • A DIVISION OF NORTH AMERICAN AVIATION, INC

TABLE C-3

## GROWTH CONSTANT-FREQUENCY DATA OBTAINED FROM B-PROPELLANT

Test No.	$P_0$ , psig	$-\alpha_b'$ , seconds $^{-1}$	$f_b$ , cps	$-\alpha_{nb}'$ , seconds $^{-1}$	$f_{nb}'$ , cps	L, inches
180	200	110.0	2260	140.0	1480	9
182	200	160.0	2170	190.0	1580	9
49	200	63.0	1120	120.0	920	15
56	200	60.0	1140	90.0	930	15
53	200	95.0	1140	98.0	890	15
179	200	8.4	410	6.8	210	41
181	200	10.0	400	15.0	230	41
183	200	12.0	400	8.3	200	41
47	400	90.0	1160	95.0	1020	15
59	400	70.0	1140	90.0	1050	15
61	400	68.0	1170	93.0	1010	15
42	400	31.0	820	50.0	720	21
50	400	60.0	820	72.0	700	21
51	400	42.0	830	53.0	720	21
64	600	49.0	1240	76.0	1100	15
54	600	50.0	840	65.0	720	21
60	600	45.0	840	63.0	770	21
62	600	36.0	850	53.0	790	21
63	600	46.0	850	60.0	750	21
72	600	36.0	860	--	--	21
73	600	40.0	840	--	--	21



ROCKETDYNE • A DIVISION OF NORTH AMERICAN AVIATION, INC.

TABLE C-4

## GROWTH CONSTANT-FREQUENCY DATA OBTAINED FROM C-PROPELLANT

Test No.	$p_o$ , psig	$-\alpha_b'$ , seconds $^{-1}$	$f_b'$ , cps	$-\alpha_{nb}'$ , seconds $^{-1}$	$f_{nb}'$ , cps	L, inches
145	200	230	2230	370	1950	9
147	200	310	2150	360	1720	9
149	200	350	2260	330	1610	9
151	200	350	2220	290	1880	9
56	200	180	1060	220	900	15
152	200	140	1260	210	1080	15
154	200	200	1240	200	1130	15
156	200	150	1270	200	970	15
158	200	180	1210	140	940	15
146	200	30	410	24	240	41
148	200	36	410	41	280	41
150	200	41	410	52	370	41
166	400	110	1220	300	1170	15
169	400	140	1510	230	1120	15
55	400	—	—	112	850	21
58	400	82	870	129	810	21
153	600	240	2400	330	2030	9
155	600	210	2320	250	2180	9
157	600	260	2260	370	1650	9
159	600	260	2320	300	2130	9
160	600	180	1350	—	—	15
161	600	140	1370	270	1120	15
162	600	160	1350	260	1130	15
165	600	120	1330	180	980	15
163	600	56	440	37	290	41
164	600	61	440	58	290	41
167	600	42	440	42	300	41
168	600	40	440	53	350	41



ROCKETDYNE • A DIVISION OF NORTH AMERICAN AVIATION, INC.

TABLE C-5

GROWTH CONSTANT-FREQUENCY OBTAINED FROM D-PROPELLANT

Test No.	$p_o$ , psig	$\alpha_b$ , seconds $^{-1}$	$f_b$ , cps	$-\alpha_{nb}$ , seconds $^{-1}$	$f_{nb}$ , cps	L, inches
75	200	10.0	1150	13.0	940	15
89	200	8.1	1130	16.0	840	15
90	200	12.0	1150	18.0	980	15
74	200	4.9	810	14.0	500	21
91	200	3.1	780	9.4	410	21
107	200	5.1	310	7.3	300	41
113	200	2.2	280	8.0	280	41

TABLE C-6

GROWTH CONSTANT-FREQUENCY DATA OBTAINED FROM E-PROPELLANT

Test No.	$p_o$ , psig	$-\alpha_b$ , seconds $^{-1}$	$f_b$ , cps	$-\alpha_{nb}$ , seconds $^{-1}$	$f_{nb}$ , cps	L, inches
103	200	37	1160	67	830	15
105	200	47	1160	67	1050	15
112	200	28	1180	91	1050	15
102	200	21	820	52	750	21
104	200	32	800	61	600	21
106	200	28	810	57	740	21

UNCLASSIFIED

Security Classification

## DOCUMENT CONTROL DATA - R&amp;D

(Security classification of title, body of abstract and indexing annotation shall be entered when the overall report is classified)

1 ORIGINATING ACTIVITY (Corporate author)	1a REPORT SECURITY CLASSIFICATION
Rocketdyne, a Division of North American Aviation, Inc., 6633 Canoga Avenue, Canoga Park, California 804	UNCLASSIFIED

2 REPORT TITLE	2b GROUP
EFFECTS OF ALUMINUM ON SOLID-PROPELLANT COMBUSTION INSTABILITY	

4 DESCRIPTIVE NOTES (Type of report and inclusive dates)

Scientific

~~CONFIDENTIAL~~ Final

5 AUTHOR(S) (Last name, first name, initial)

Oberg, C. L.; Huebner, A. L.

6 REPORT DATE	7a. TOTAL NO. OF PAGES	7b. NO. OF REFS
30 July 1966	109	42
8a. CONTRACT OR GRANT NO.	9a. ORIGINATOR'S REPORT NUMBER(S)	
AF49(638)-1575	R-6654	
9 PROJECT NO.	9b. OTHER REPORT NO(S) (Any other numbers that may be assigned this report)	
61445014	AFOSR 66-1847	
10 AVAILABILITY/LIMITATION NOTICES	11a. SPONSORING MILITARY ACTIVITY	
3. Each transmittal of this document outside the agencies of the U. S. Government must have prior approval of AFOSR (SRGL).		
11b. SPONSORING MILITARY ACTIVITY		
Air Force Office of Scientific Research Arlington, Virginia 22209		

12 ABSTRACT An analytical and experimental program to investigate the effects of aluminum on solid-propellant combustion instability was conducted. The analytical phase was devoted to a determination of the energy dissipation rate associated with possible damping mechanisms. The relative magnitude of these damping mechanisms are developed and discussed. The effects of aluminum on non-acoustic instability were also considered in the analytical phase. It is shown that the nonacoustic problem could be treated by employing conventional acoustic methods. This information was used to propose a mechanism for quasi-periodic shedding of aluminum from the burning surface. This analysis was followed by an experimental phase. Measurements were made employing a T-burner in which a pressure pulse could be generated. Measurements were made on propellants containing up to 15-percent aluminum at mean-pressure levels up to 600 psi and over a frequency range of 200 to 2000 cps. A discussion is presented of the results of these experiments, particularly with respect to the damping mechanisms considered in the analysis. Some information applicable to nonacoustic instability was obtained as well. (U)

**UNCLASSIFIED**

Security Classification

KEY WORDS

Aluminum  
Solid-Propellants  
Combustion Instability  
Particulate Damping  
Droplet Deformation

**INSTRUCTIONS**

**1. ORIGINATING ACTIVITY:** Enter the name and address of the contractor, subcontractor, grantee, Department of Defense activity or other organization (corporate author) issuing the report.

imposed by security classification, using standard statements such as:

- (1) "Qualified requesters may obtain copies of this report from DDC."
- (2) "Foreign announcement and dissemination of this report by DDC is not authorized."
- (3) "U. S. Government agencies may obtain copies of this report directly from DDC. Other qualified DDC users shall request through"
- (4) "U. S. military agencies may obtain copies of this report directly from DDC. Other qualified users shall request through"
- (5) "Distribution of this report is controlled. Qualified DDC users shall request through"

If the report has been furnished to the Office of Technical Services, Department of Commerce, or sale to the public, indicate that and enter the price, if known.

**11. APPROVAL/NOTIFY NOTES:** Use for additional explanatory notes.

**12. SPONSORING ACTIVITY ACTIVITY:** Enter the name of the department, agency, office, or laboratory sponsoring (paying for) the research and/or development. Include address.

**13. ABSTRACT:** Enter an abstract giving a brief and factual summary of the documentation of the report, even though it may not appear elsewhere in the body of the technical report. If additional space is required, a continuation sheet should be attached.

It will be desirable that the abstract of classified reports be brief and to the point, giving the classification and the information in the report which represents the TSU. (See TSU)

The abstract should be typed on a separate sheet, if necessary, or on the first page of the report.

**14. LINE NUMBER:** Use for identification of each page.

Each page should be numbered consecutively.

Each page should be numbered consecutively.

Each page should be numbered consecutively.

Each page should be numbered consecutively.